

CRANFIELD UNIVERSITY

RONGXIN XU

Optimal Design of a Composite Wing Structure for a Flying-Wing
Aircraft Subject to Multi-constraint

School of Engineering

Aerospace Engineering

Aircraft Design Programme

MSc by Research
Academic Year: 2011 - 2012

Supervisor: SHIJUN GUO
JANUARY 2012

CRANFIELD UNIVERSITY

SCHOOL OF ENGINEERING

Aerospace Engineering
Aircraft Design

MSc by Research

Academic Year 2011 - 2012

RONGXIN XU

Optimal Design of a Composite Wing Structure for a Flying-Wing
Aircraft Subject to Multi-constraint

Supervisor: SHIJUN GUO

JANUARY 2012

© Cranfield University 2012. All rights reserved. No part of this
publication may be reproduced without the written permission of the
copyright owner.

ABSTRACT

This thesis presents a research project and results of design and optimization of a composite wing structure for a large aircraft in flying wing configuration. The design process started from conceptual design and preliminary design, which includes initial sizing and stressing followed by numerical modelling and analysis of the wing structure. The research was then focused on the minimum weight optimization of the composite wing structure subject to multiple design constraints. The modelling, analysis and optimization process has been performed by using the NASTRAN code. The methodology and technique not only make the modelling in high accuracy, but also keep the whole process within one commercial package for practical application.

The example aircraft, called FW-11, is a 250-seat commercial airliner of flying wing configuration designed through our MSc students Group Design Project (GDP) in Cranfield University. Started from conceptual design in the GDP, a high-aspect-ratio and large sweepback angle flying wing configuration has been adopted. During the GDP, the author was responsible for the structural layout design and material selection. Composite material has been chosen as the preferable material for both the inner and outer wing components. Based on the derivation of structural design data in the conceptual phase, the author continued with the preliminary design of the outer wing airframe and then focused on the optimization of the composite wing structure.

In the preliminary design phase, classical method based on statistical design data was used to calculate the initial size of the main structural components at first. Since this classical technique is always thought to be conservative for initial design, advanced numerical analysis method, finite element method (FEM), is subsequently used to update the initial design result.

In the optimization process, attention was mainly focused on the thickness and layup of the laminated upper and lower stiffened skin panels, which make significant influence to the structure weight and stiffness. The optimization was based on the finite element model of the outer wing box. The objective was to

minimize the structure weight. Multiple constraints include failure criterion related to laminate strength, allowable design limiting strain covering damage tolerance, minimum flutter speed reflecting dynamic aeroelastic stability and minimum percentage of each ply orientation considering load condition uncertainties.

For design variables, a pre-process was adopted by setting the laminate in blocks regardless the stacking sequence. This allows the laminate thickness change discretely in the scale of each lamina thickness and makes the optimization practical and efficient. As a result, a structure weight reduction by 7.7% was achieved for the whole outer wing airframe by only optimising the laminated skins.

At the end, a post-process was added to arrange the laminate stacking sequence according to the optimization result. This final result has also proved the optimization mentioned above is applicable.

In conclusion, the methodology and technique developed in this research has demonstrated a practical and user friendly approach for aircraft structure optimization. The whole process can be kept within one commercial package including high fidelity modelling and high accuracy analysis and also optimization with multiple design constraints.

Keywords:

Structural Design, Multidisciplinary Optimization, Finite Element, Aeroelasticity, Flutter, Failure Criterion, NASTRAN

ACKNOWLEDGEMENTS

I express my sincere gratitude, regards and thanks to my supervisor Dr. Shijun Guo for his excellent guidance, invaluable suggestions and generous help at all the stages of my individual research work.

I would like to give my appreciation to Prof. John Pieliding, Prof. Howard Smith and other staff of Department of Aerospace Engineering for their best instructions throughout the group design project. And thanks to all my classmates for their hard work and perfect cooperation during the project.

Thank you to Faliang Wang, Chao Tong and Jin Zhang for sharing the aerodynamic and inertial load data.

Thank you to Dr. Rui Pires for his lecture on practical finite element analysis.

Thank you to Dr. Daochun Li and Dr. Qiang Fu for providing help on my NASTRAN studying.

Thanks to my company AVIC and also CSC for providing me this opportunity and sponsorship for studying at Cranfield University.

Finally, thanks to my wife Li and my parents for their support and love and taking care of my lovely daughter Yuanyuan in my absence.

TABLE OF CONTENTS

ABSTRACT	i
ACKNOWLEDGEMENTS.....	iii
TABLE OF CONTENTS	v
LIST OF FIGURES.....	vii
LIST OF TABLES	viii
LIST OF EQUATIONS.....	viii
NOTATIONS	xi
1 Introduction	1
1.1 Background.....	1
1.2 Aim and Objectives	3
2 Literature Review	5
2.1 Analysis of Composite Structures.....	5
2.2 Flutter Analysis for Wing Structure.....	6
2.3 Optimization of Composite Structure.....	8
3 Theory and Methodology.....	13
3.1 Composite Failure Theory.....	13
3.1.1 Tsai-Hill Theory.....	13
3.1.2 Hoffman Theory.....	13
3.1.3 Tsai-Wu Theory	14
3.2 Flutter Analysis Theory.....	14
3.3 Optimization Theory	16
3.4 Methodology.....	17
3.4.1 Design Methods.....	17
3.4.2 Optimization.....	18
3.4.3 Design Tools.....	20
4 Derivation of Structural Design Data	23
4.1 Wing Geometry and Specification	23
4.2 Load Analysis.....	24
4.3 Material Selection.....	29
5 Structural Layout Design.....	33
5.1 General View.....	33
5.2 Inner Wing Structure Concept	33
5.3 Outer Wing Structural Layout.....	35
6 Classical Initial Sizing.....	37
6.1 Composite Material Property Estimation	37
6.2 Structure Member Initial Sizing	39
6.2.1 Spar Webs.....	40
6.2.2 Composite Skin.....	41
7 Finite Element Approach Estimation	45
7.1 Static Analysis.....	45
7.1.1 FE Structure Modelling	45
7.1.2 Distributed Loads Definition.....	48
7.1.3 Static Analysis Results	49
7.2 Aeroelastic Analysis	53
7.2.1 Modelling for Dynamic Analysis.....	53

7.2.2	Flutter Analysis Modelling.....	56
7.2.3	Flutter Analysis Results	59
8	Optimization	63
8.1	Optimization Model Description.....	63
8.2	Optimization Pre-process	64
8.2.1	Design Variable Definition	64
8.2.2	Response and Constraint Definition	67
8.2.3	Optimization Constraints Definition.....	68
8.3	Optimization Results	69
8.3.1	Optimization Process.....	69
8.3.2	Optimization Results Analysis.....	71
8.4	Laminate Post-process.....	76
9	Discussion and Future Work	79
9.1	Discussion.....	79
9.2	Future Work	80
10	Conclusion	83
	REFERENCES.....	85
	APPENDICES	89

LIST OF FIGURES

Figure 2-1 A Flow-chart of the GA Procedure [20]	10
Figure 3-1 Structure Design Requirements	19
Figure 4-1 Three-view Drawing of FW-11	23
Figure 4-2 Flying Wing Aircraft Loads Condition	25
Figure 4-3 Span-wise Lift Distribution for Level Flight	25
Figure 4-4 Span-wise Mass Distribution	26
Figure 4-5 Shear Force Diagram.....	27
Figure 4-6 Bending Moment Diagram	27
Figure 4-7 Torque Diagram	28
Figure 4-8 FW-11 Material Breakdown.....	30
Figure 5-1 Main Structure Layout.....	33
Figure 5-2 Inner Wing Structure Layout	34
Figure 5-3 Outer Wing Structure Layout.....	36
Figure 6-1 Dimensions of Wing Structural Box.....	39
Figure 6-2 Design Zones of the Outer Wing.....	42
Figure 7-1 Advanced Meshing in CATIA	45
Figure 7-2 Composite Laminate Modelling in Patran.....	47
Figure 7-3 Numerical Model for Static Analysis.....	48
Figure 7-4 Initial Deformation Result	49
Figure 7-5 Initial FI Result of Laminated Skin.....	50
Figure 7-6 Initial Strain Result of Laminated Skin.....	51
Figure 7-7 Typical Strain Level for CFRP [8].....	52
Figure 7-8 Initial Strain Result of Substructure	53
Figure 7-9 Mass of Control Surfaces	54
Figure 7-10 Interference Vibration Modes	55
Figure 7-11 Natural Frequency Modes.....	56
Figure 7-12 FE Method of Aeroelastic Analysis.....	57
Figure 7-13 Aerodynamic Model using DLM	58
Figure 7-14 Structural-Aerodynamic Connection.....	59
Figure 7-15 V-g and V-f Curves for Initial Design	60
Figure 8-1 Laminate Block Definition.....	65
Figure 8-2 Laminate Modelling in Block	66
Figure 8-3 Structural Optimization Flow Chart.....	69
Figure 8-4 Optimization History	70
Figure 8-5 Wing Deflection after Optimization	72
Figure 8-6 Optimized FI Result of Laminated Skin	73
Figure 8-7 Optimized Strain Result of Laminated Skin.....	74
Figure 8-8 V-g and V-f Curves for Optimized Design	75
Figure 8-9 Critical V-g Curves for Optimization Comparison.....	76
Figure 8-10 Laminate Post-process Analysis	77
Figure 9-1 ABD Matrices Comparison.....	80

LIST OF TABLES

Table 3-1 Stage Tasks and Tools.....	21
Table 4-1 Geometry Parameter of FW-11	23
Table 4-2 Specification of FW-11	24
Table 4-3 Material Properties of T300/N5208.....	30
Table 6-1 Skin Laminate Thickness in Initial Design	43
Table 7-1 Finite Element Statistics	46
Table 7-2 Calculated Equivalent Elastic Constants	47
Table 7-3 Inputs and Outputs for Flutter Analysis	56
Table 8-1 Design Constraints.....	68
Table 8-2 Structure Weight Comparison	71
Table 8-3 Laminate Optimized Design	71
Table 8-4 Optimization Post-process for Zone2	77

LIST OF EQUATIONS

(3-1).....	13
(3-2).....	14
(3-3).....	14
(3-4).....	15
(3-5).....	15
(3-6).....	16
(3-7).....	16
(3-8).....	16
(3-9).....	16
(3-10).....	16
(3-11).....	17
(3-12).....	17
(3-13).....	17
(6-1).....	38
(6-2).....	38
(6-3).....	38
(6-4).....	38
(6-5).....	39
(6-6).....	40
(6-7).....	40
(6-8).....	40
(6-9).....	40
(6-10).....	40
(6-11).....	40
(6-12).....	40
(6-13).....	40

(6-14).....	41
(6-15).....	41
(6-16).....	41
(6-17).....	41
(7-1).....	58
(7-2).....	61
(8-1).....	63
(8-2).....	66
(8-3).....	68
(8-4).....	68
(8-5).....	68

NOTATIONS

Mathematical symbols

$A_{jj}(m, k)$	Aerodynamic influence coefficient matrix
B_{hh}	Modal damping matrix
\bar{c}	Reference semichord
d	A feasible direction
E_1	Longitude Young's Modulus, GPa
E_2	Transverse Young's Modulus, GPa
g	Structural damping coefficient
G_{12}	Shear Modulus, GPa
$I^{(t)}$	Active constraints space
k	Reduced frequency
K_{hh}	Modal structural stiffness matrix
m	Mach number
M_{hh}	Modal mass matrix
P_k	Forces at aerodynamic grid points
Q_{hh}^I	Modal aerodynamic damping matrix
Q_{hh}^R	Modal aerodynamic stiffness matrix
S	Shear Strength, MPa
t	Laminate thickness, mm
u_k	Displacements at aerodynamic grid points
$\{u_h\}$	Modal amplitude vector
V	Velocity
X_t	Longitudinal Tensile Strength, MPa
X_c	Longitudinal Compressive strength, MPa
Y_t	Transverse Tensile Strength, MPa
Y_c	Transverse Compressive Strength, MPa

α^*	Scalar move parameter
γ	Transient decay rate coefficient
θ	Ply orientation
λ_j	Lagrange multiplier
ν_{12}	Poisson's Ratio
ρ	Density, kg/m ³
σ_1	1-direction stress
σ_2	2-direction stress
σ_x	Laminate x-direction stress
σ_y	Laminate y-direction stress
σ_b	Allowable direct stress
σ_s	Allowable shear stress
τ_{12}	Ply shear stress
τ_{xy}	Laminate shear stress
ω	Circular frequency

Abbreviations

CAD	Computer Aided Design
CAE	Computer Aided Engineering
CFRP	Carbon Fibre Reinforced Plastic
DLL	Design Limit Load
DLM	Doublet-Lattice Method
DOF	Degrees of Freedom
DUL	Design Ultimate Load
EAS	Equivalent Air Speed
FE	Finite Element
FI	Failure Index
GA	Genetic Algorithm
GD	Gradient-based Deterministic Method

GDP	Group Design Project
MTOW	Maximum Take-off Weight
TAS	True Air Speed

1 Introduction

1.1 Background

This research project started from a novel conceptual design of a 250-seat commercial airliner FW-11 in a student Group Design Project (GDP). As part of a training cooperation programme between AVIC (Aviation Industry Corporation of China) and Cranfield University, this aircraft design is divided into three stages: Conceptual Design (2011), Preliminary Design (2012), and Detailed Design (2013), and will be completed by three different cohorts of students from AVIC each year.

The target of the GDP is to design a long range flying wing passenger aircraft to meet the increasing global air traffic demand. The design philosophy of FW-11 is low fuel consumption and low noise emission. In order to achieve this target, the conventional aircraft configuration seems to be close to its limits. Alternative configurations were investigated. Flying wing layout seems to offer promising benefits in terms of efficiency.

“A flying wing is a tailless fixed-wing aircraft which has no definite fuselage, with most of the crew, payload and equipment being housed inside the main wing structure.” [1] Theoretically, a clean flying wing is the most aerodynamically efficient design configuration for a fixed wing aircraft. It also offers high structural efficiency for a given wing depth, leading to light weight and high fuel efficiency. Therefore, flying wing morphology will probably become an attractive choice for the design of future large aircraft.

Carbon Fibre Reinforced Plastic (CFRP) materials have many advantages over aluminium alloys, especially in specific stiffness and strength, fatigue resistance, laminate tailoring and some manufacturing flexibilities. Nowadays, the percentage of composite materials in the structure of modern aircraft has been keeping increasing significantly. Consequently, CFRP is selected as the preferred material in the FW-11 wing structure design.

However, due to the anisotropic nature, the analysis of composite material structure is more complex than metallic structure. One of the major differences in composite analysis, as opposed to metal, is that strain is the major concern and not stress. Composite structures are made up of different plies, and each ply will be stressed at a different level because the ply's elastic modulus is dependent upon the ply orientation.

In modern aircraft design, to get an optimal result as much as possible is very important for designers, especially in the early conceptual or preliminary design stage. That will significantly reduce the design risk and cost in detail design stage. As the development of numeric technology and the multidisciplinary optimization theory, the optimal design for large aircraft structures has become feasible. In this report, the author focused on the optimal design research for the laminated skins of a wing structure in preliminary design phase.

Structure weight has always been important for designers. Any saving of structural weight can lead to a corresponding increase in payload. Alternatively, for a given payload, saving in aircraft weight means reduced power requirement. Hence, at this preliminary design stage, structure weight has been set as the optimization objective.

For design constraints, the task of structure design should meet a lot of requirements such as strength, stiffness, fatigue, damage tolerance, manufacture etc. Moreover, as the flight speed keeps increasing, it is important for designers to concern aeroelastic problem in modern aircraft design. FW-11 is designed with a subsonic cruising speed. In the conceptual design stage of this project, a high-aspect-ratio wing with large sweepback angle configuration has been adopted, and the wing boasts large deformation due to flight load. Under this situation, the coupling of stiffness between bending and torsion is intensified and make the aeroelastic problem more severe. In addition, the application of CFRP materials also makes some design requirements different from traditional metallic structures.

In GDP work, the author was mainly in charge of structure layout design and material selection. Based on some inputs from conceptual design, the author's IRP work started practically after GDP work. Attention was then paid to the optimal design of the composite outer wing structure subject to multi-constraint including strength, damage tolerance, dynamic aeroelastic stability and other practical considerations.

In this thesis, an introduction was presented initially, including background, and research objectives. Secondly, the bibliography work that had been done by the author before the practical stage of research was shown. Then some related theories were mentioned to guide the analysis and optimization work. After the investigation of the methods and theories used by others in related field, the methodology was chosen for this example by the author. The following chapters were the practical design and optimization work. At last, discussion was made based on the results and the future work was included.

1.2 Aim and Objectives

This research project is aimed at optimal design of the wing structure for a 250-seat flying-wing aircraft. For the initial design, both classic and advanced numerical approaches are used in this stage to validate the method availability mutually. In order to get an optimal design, optimization based on the numerical model for minimum structure weight is a feasible choice. The dimensions and layout of the composite skin panels will be analysed and optimised subject to several constraints.

By optimising the composite skin, a minimum structure weight saving of 7% should be achieved for the whole outer wing structure.

The research work is divided into several stages with objectives as follows:

1. Complete GDP work and get the derivation data for structure design;
2. Structure layout design of the whole wing structure of FW-11 in GDP;
3. Initial sizing for the main components of the composite outer wing structure;

4. Create an analytical and numerical model of the outer wing structure;
5. Carry out static strength and stiffness analysis for initial design;
6. Carry out dynamic flutter analysis;
7. Optimization for composite skin panels subject to multi-constraint;
8. Discussion and thesis writing up.

The modelling, analysis and optimization process has been performed by using the NASTRAN code. The methodology and technique not only make the modelling in high accuracy, but also keep the whole process within one commercial package for practical application.

2 Literature Review

2.1 Analysis of Composite Structures

Composite materials have an extremely large group. However, carbon fibre-reinforced plastic (CFRP) laminates are most widely used in aircraft design, because laminate theory is getting very sophisticated in both macromechanics and micromechanics nowadays. Composite structures, compared with conventional metallic structures, are more complex on structure analysis because they have more independent constants of properties. Generally, there are two main methods to analyze composite structures: classical analysis and finite element analysis.

Classical methods of analyses are based on the application of the equations of equilibrium and compatibility, together with the stress-strain relations for the material, to produce governing equations which must be solved to obtain displacements and stresses. [2]

The major procedures of the classical strength analysis of laminated FRP structures are shown below:

- 1) Calculate the equivalent engineering elastic constants for each laminate of the structure by using laminate theory;
- 2) Work out the 'averaged' stress of the structure subjected to external loads;
- 3) Figure out the force and moment from the above 'averaged' stress and go back to the laminate theory for strain;
- 4) Calculate the 'local' stress in fibre and matrix in each ply for strength evaluation.

However, classical methods are limited to simple geometries and 'real' structural features. As we move away from simple situations, the governing equations become increasingly complicated and require ever-more

sophisticated mathematical techniques to solve them. Finite element (FE) method is an alternative approach to solve the governing equations of a structural problem. A typical finite element analysis has three main procedures: preparing FE modelling, performing calculation, and post-process.

Most composite structures are best modelled using plate and shell finite elements. These have to be modified to allow for laminated materials. In particular, the strains have to be expressed in terms of mid-plane strains and curvatures. [2]

However, both classical and FE methods need large amount of calculations when the composite structure was designed complicatedly. Fortunately, in practical engineering, engineers usually design laminated structure as simple as possible due to manufacturing consideration. The ultimate objective of design is the emergence of an acceptable final product. Less obvious but just as important, a structure must not be so complex or difficult in concept that its realization will create great difficulties, or increase the cost of the manufacturing process. Practically, engineers usually design laminated composite panels in symmetric and balanced format using four standard angles of 0° , 45° , -45° and 90° . This will also make the analysis of composite structure easier.

2.2 Flutter Analysis for Wing Structure

Flutter is a phenomenon where the interaction between the aerodynamic forces, structural characteristics, and inertias results in an oscillation. Flutter is essentially a dynamic aeroelastic stability problem. For a wing lifting surface, there are mainly two types of flutter: classical bending-torsion flutter and control surface flutter. However flutter analysis is always a complicated job. Some investigations had been done by the author before the practical work started.

At the beginning and long term of the aeroelastic mechanics research, the aircraft structure being idealised as a one-dimensional beam system is a necessary and basic hypothesis for flutter analysis. And even in modern period, satisfactory results can also be achieved in many circumstances.

Gabriel A. Oyibo [3] carried out the flutter analysis by simplifying a wing as a cantilevered flat plate-like lifting surface in an incompressible airflow. This idealization can obviously reduce the quantity of degrees of freedom in analysis. Meanwhile, an unsteady aerodynamic load and the uncoupled bending and torsional frequencies are employed in flutter analysis. This generalized theory of flutter analysis has a good exposure of the interactions between aerodynamics and elastic structures and makes the flutter analysis more efficient.

Nowadays, finite element method is commonly applied in aeroelastic analysis. Aerodynamic and structural analyses can be both based upon FE approach and two FE models are needed. Lifting surface model calculates unsteady aerodynamic forces, while structural model provide elastic and inertial characteristics. These two models are developed independently and then connected together by numerical interpolation method. At last, discrete method is used to solve the flutter equation of motion. [4]

There are no method and theoretical differences on flutter analysis between composite wing and metallic wing. However, the anisotropic nature of composite material property has significant influence on flutter characteristics.

During the research by Cole, Nagaraja and Rivera [5], a finite-element model of composite wing was generated to perform flutter analysis for the purpose of comparing with flutter test result. All components of the wing structure were modelled with composite laminates. And the wing mass was distributed to the nodes of the model. As a result, the analysis and test results are very close.

In the research done by Chowdary, Parthan and Sinha [6], quadratic isoparametric elements were used to establish the finite element model in order to estimate the flutter characteristics for a laminated panel. Some parameters, such as ply orientations, stacking sequences and so on are discussed. The conclusion illustrates that the flutter speed can be significantly increased if the fibre orientations coincide with the airflow direction. The analysis result also shows that the coupling effects due to anisotropy of laminates have great effect

on the flutter characteristics. The effect will get more pronounced if the panel has fewer layers.

Qin, Marzocca and Librescu [7] developed a unified aeroelastic model to perform flutter instability and aeroelastic response analysis at compressible subsonic flight speed. An asymmetric lay-up composite thin-walled beam was modelled to simulate the elastic coupling effect for aircraft wings. The aerodynamic model was based on 2-D strip theory. The result indicated that elastic tailoring and warping restraint play a considerable role on flutter.

2.3 Optimization of Composite Structure

The directional nature of composite laminae provides the ability to construct a material which can meet specific loads and/or stiffness requirements without wasting material by providing strength and stiffness where they are not needed. [8] Therefore, composite materials offer a great potential and many advantages in the optimization of aircraft structures.

However, this advantage also makes the optimization of composite structure more challenging. Compared with traditional metallic materials, anisotropic composites have much more design variables which all have significant influence on structure characteristics. For laminated panels that are most widely used in aircraft structures, ply thickness, fibre orientation angles and stacking sequences are the most important variables which can be optimised by the designers.

In order to make the optimization easier, some simplifications should be applied. Early in the 1970s, Schmit and Farshi [9] had done some optimization work on homogeneous and orthotropic property laminated composites. The ply thicknesses were regarded as continuous variables, and the optimization was considered as a series of linear problems.

Nowadays, the FE method is widely used in the optimization of composite structures. Almeida [10] and Walker [11] both associated the FE optimization technique with GA method, and a simple composite plate was used to

demonstrated it. In the research done by Honda [12], numerical method provided accurate optimization solution for the stacking sequence of vibrating composite plate. Other researches using simple composite plates to perform FE method of optimization were performed by Kere [13] and Zehnder [14].

In practical engineering, an optimal design should meet all kinds of design constraints. For composite structure, strength in terms of failure mechanism is usually the most important one. Different failure criteria, such as maximum stress, Tsai-Wu and so on, were taken into account by Narayana [15] and Lopez [16].

All researches mentioned above selected simple composite plates to demonstrate the optimization technique. However, FE method also makes the optimization of large composite wing structure possible. Wang, Williams and Llamas [17] performed a structural optimization for an aircraft wing with manufacturing considerations. In this paper, a traditional design and optimization for an aircraft wing without considering composite manufacturability was performed firstly. The wing was divided into a number of optimization zones in order to achieve the minimum weight subject to strength constraint. However, in aircraft industry, the complexity of the wing skin thickness distribution is of great concern to the manufacturer. Then the author focused on incorporating manufacturing constraints into optimization with respect to manufacturing complexity requirements.

Liu, Toropov, Quein and Barton [18] employed a bi-level method to optimize the stiffened panels of a composite wing subject to manufacturing constraints. At panel level, the optimization work was focused on the cross section dimensions of the panel. While at laminate level, the laminate thickness and stacking sequence of plies was optimised. At last, a considerable structure weight reduction was obtained and the best stacking sequence was achieved under deflection and manufacturing constraints for laminated composite wing structures.

Structural optimization usually aims to get minimum structure weight. However, when tailoring the composite directional property, weight has little change. Other structure performances should be set as the objective. Aeroelastic characteristic is usually concerned in such type of optimization. Dr. Guo contributed a series of investigations on composite wing structure optimization.

Guo, Bannerjee and Cheung [19] carried out an aeroelastic optimization of a composite wing, and studied the effect of laminate rigidities on flutter speed. The conclusion demonstrated that the torsion and coupling rigidity had more significant effects than bending rigidity, and optimizing the fibre orientations was the best choice to achieve maximum flutter speed without any weight penalty.

Dr. Guo also used different optimization algorithms to perform composite wing structure optimizations to achieve maximum flutter speed. In these researches [20-21], two different optimization methods: gradient-based deterministic method (GD) and genetic algorithm (GA) were investigated to make a comparison. The conclusion shows that GD requires less computer time but largely depends on initial laminate lay-up. By contrast, GA needs more computing time but is preferable for its robustness of achieving an optimum solution.

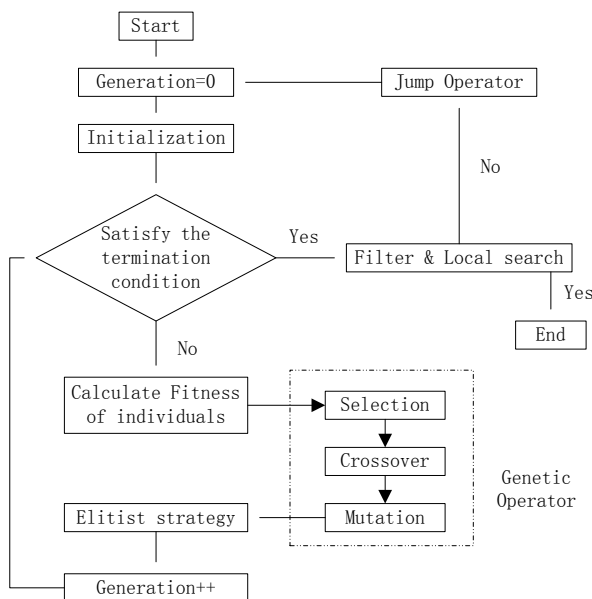


Figure 2-1 A Flow-chart of the GA Procedure [20]

Another frequently used method in flutter optimization for composite wing structure is called dynamic stiffness method (DSM). Lillico, Butler, Guo, and Banerjee [22] obtained the bending, torsion, and coupling rigidities based on the composite wing geometry, properties, and laminate layups. Then by solving the governing equation, the rigidities were optimized.

In order to make full use of the advantages of composite in structural optimization, a two-stage multi-objective optimization was developed by Dr. Guo [23-24]. The first stage was focused on the minimum weight optimization subject to multiple constraints. Laminate thickness was taken as design variables. Based on this minimum weight composite structure, the second stage was then focused on increasing flutter or aeroelastic response features.

3 Theory and Methodology

3.1 Composite Failure Theory

For the strength analysis of FRP material, there are generally five failure criteria in macro mechanics:

- (1) Maximum stress theory,
- (2) Maximum strain theory,
- (3) Tsai-Hill theory,
- (4) Hoffman theory, and
- (5) Tsai-Wu theory.

These failure theories are all based on such assumptions: macroscopic homogeneity, small deformation and linear elasticity, equal modulus in compression and tension, and plane stress. The first two theories are called non-interactive theories, while the last three are interactive theories which are more commonly used. In this report, only the last three failure criteria for stress-based theory are introduced.

3.1.1 Tsai-Hill Theory

Ply failure would occur if $F.I. \geq 1$ [25]:

$$F.I. = \left(\frac{\sigma_1}{X}\right)^2 + \left(\frac{\sigma_2}{Y}\right)^2 + \left(\frac{\tau_{12}}{S}\right)^2 - \frac{\sigma_1\sigma_2}{X^2} \quad (3-1)$$

Where X and Y are absolute value of tensile or compressive strength depending upon σ_1 and σ_2 .

3.1.2 Hoffman Theory

Ply failure would occur if $F.I. \geq 1$ [25]:

$$F.I. = F_1\sigma_1 + F_2\sigma_2 + F_{11}\sigma_1^2 + F_{22}\sigma_2^2 + F_{33}\tau_{12}^2 + 2F_{12}\sigma_1\sigma_2 \quad (3-2)$$

Where $F_1 = \frac{1}{X_t} - \frac{1}{X_c}$, $F_2 = \frac{1}{Y_t} - \frac{1}{Y_c}$, $F_{11} = \frac{1}{X_t X_c}$, $F_{22} = \frac{1}{Y_t Y_c}$, $F_{33} = \frac{1}{S^2}$,

$$F_{12} = \frac{-1}{2X_t X_c}$$

The five basic failure strengths X_t , Y_t , X_c , Y_c , S for a FRP ply are part of material properties from manufacturer which are measured from a specially orthotropic ply in material axes.

3.1.3 Tsai-Wu Theory

Ply failure would occur if $F_I \geq 1$ [25]:

$$F.I. = F_1\sigma_1 + F_2\sigma_2 + F_6\tau_{12} + F_{11}\sigma_1^2 + F_{22}\sigma_2^2 + F_{66}\tau_{12}^2 + 2F_{12}\sigma_1\sigma_2 \quad (3-3)$$

Where $F_1 = \frac{1}{X_t} - \frac{1}{X_c}$, $F_2 = \frac{1}{Y_t} - \frac{1}{Y_c}$, $F_{11} = \frac{1}{X_t X_c}$, $F_{22} = \frac{1}{Y_t Y_c}$, $F_{33} = \frac{1}{S^2}$,

$$F_{12} = \frac{F_{12}^*}{\sqrt{F_{11} F_{22}}}$$

F_{12}^* (≈ -0.5) is a term to be determined by a biaxial test. The fact

that the shear strength in principal material coordinates is independent

of shear stress sign will lead to $F_6 = 0$, $F_{66} = \frac{1}{S^2}$.

3.2 Flutter Analysis Theory

Flutter is the dynamic aeroelastic stability problem. Harmonic motion is the critical situation of the stable oscillation. Therefore, the basic equation of harmonic motion is valid only at flutter [4]. It is performed using modal coordinates and based on linear case assumption. The unsteady aerodynamics of a harmonic oscillating lifting system is included.

$$\left[M_{hh} p^2 + B_{hh} p + K_{hh} - \frac{1}{2} \rho V^2 Q_{hh}(m, k) \right] \{u_h\} = 0 \quad (3-4)$$

Where M_{hh} is modal mass matrix, B_{hh} is modal damping matrix, K_{hh} is modal stiffness matrix, m is Mach number, k is reduced frequency, $Q_{hh}(m, k)$ is aerodynamic force matrix for a specific Mach number and reduced frequency, p is eigenvalue, ρ is fluid density, V is velocity, and u_h is modal amplitude vector.

The solution of this equation involves a series of complex eigenvalue solutions. Generally, there are three methods of flutter solution techniques: K-method, KE-method, and PK-method. The eigenvalue problem to be solved by different methods depends on the way in which the aerodynamic loads are included in the equations of motion or whether certain damping terms are included.

The K-method computes eigenvalues and vectors for user-specified reduced frequencies. It introduces the aerodynamics into a vibration analysis as complex inertial terms and introduces an artificial complex structural damping, proportional to the stiffness, to sustain the assumed harmonic motion.

The KE-method is an efficient K-method. It computes eigenvalues but does not support a viscous damping matrix B_{hh} .

The PK-method computes eigenvalues and vectors for user-specified velocities. This approach introduced the aerodynamic loads into the equations of motion as frequency dependent stiffness and damping terms. The basic equation for PK-method is [4]

$$\left[M_{hh} p^2 + \left(B_{hh} - \frac{1}{4} \rho \bar{c} V Q_{hh}^I / k \right) p + \left(K_{hh} - \frac{1}{2} \rho V^2 Q_{hh}^R \right) \right] \{u_h\} = 0 \quad (3-5)$$

Where the new terms Q_{hh}^I is modal aerodynamic damping matrix, Q_{hh}^R is modal aerodynamic stiffness matrix, \bar{c} is reference length.

The matrices are all real, because the complex aerodynamic terms are split into real and imaginary terms. The complex eigenvalue solution of the PK-method equation of motion is

$$p = \omega(\gamma \pm i) \quad (3-6)$$

Where ω is circular frequency = $2\pi f$, γ is transient decay rate coefficient. The structural damping coefficient is expressed as the decay rate coefficient.

$$g = 2\gamma \quad (3-7)$$

Flutter occurs for values of ρ , m , and V for which $g = 0$.

3.3 Optimization Theory

A constrained optimization problem can be generally expressed in the following form. Finding a set of parameters, $X = \{x_1, x_2, \dots, x_n\}$, to minimize or maximize the objective function $F(X)$, subjected to

$$g_j(X) \geq 0 \quad j = 1, \dots, n_g \quad \text{inequality constraints} \quad (3-8)$$

$$h_k(X) = 0 \quad k = 1, \dots, n_h \quad \text{equality constraints} \quad (3-9)$$

$$x_i^L \leq x_i \leq x_i^U \quad i = 1, \dots, n \quad \text{side constraints} \quad (3-10)$$

The objective function is the scalar quantity to be minimized or maximized. It is a function of the set of design variables. Side constraints are placed on the design variables to limit the region of search. The inequality constraints are expressed in a greater than or equal to zero form by convention; that is, a constraint is satisfied if its value is positive. Equality constraints, if present, must be satisfied exactly at the optimal design.

The optimization algorithms in MSC.Nastran belong to the family of methods generally referred to as “gradient-based,” since, in addition to function values, they use function gradients to assist in the numerical search for an optimum.

$$X^{q+1} = X^q + \alpha^* S^q \quad (3-11)$$

Where q is iteration number, S is search direction, and α^* is scalar move parameter. The $\alpha^* S^q$ is the design modification at current step and α^* is the step length that yields the search direction defined by S .

In constrained optimization problems, design points that satisfy Kuhn-Tucker conditions are likely in the area of optimum results. The governing equation is the stationary condition of the Lagrange function:

$$L(X, \lambda) = F(X) + \sum_{j=1}^M \lambda_j g_j(X) \quad (3-12)$$

$$\lambda_j \geq 0 \quad (3-13)$$

Where λ_j is Lagrange multiplier.

The optimization algorithms in MSC.Nastran belong to the family of methods generally referred to as “gradient-based,” since, in addition to function values, they use function gradients to assist in the numerical search for an optimum.

3.4 Methodology

3.4.1 Design Methods

In this research, the whole structure design process was divided into several stages including structural layout design, initial sizing, static analysis, and flutter analysis.

After the literature review work, a certain number of methods were found to carry out each job in different stages. It is important to find proper methods for this example.

In the structural layout design phase, M Niu [26] and Denis Howe [27] both provide some practical techniques. While M Niu supplies more statistical design

data which is valuable for making decision of some important design parameters.

In initial sizing stage, Denis Howe's method [27] is easy to perform and is suitable for early design stage. It provides simple experienced equations which have taken comprehensive design requirements into account. Before calculate the initial sizes of the structure main parts, the material allowable value should be estimated. It is a complex job especially for composite material due to its directional property characteristic. A useful guide and simple method for evaluating laminate strength is the '10-percent rule' proposed by H Smith [28].

The classical calculations involved in the early design stage are commenced manually. Although the classical methods are getting more and more sophisticated in modern aircraft design, they are still approximate sciences and usually conservative and over-estimated. Therefore, in the following analysis stages, an advanced numerical method is used to update the initial design result. Probably the most widely used tool in structural analysis is the use of finite element (FE) method.

In FE static analysis, Tsai-Wu [29] failure criterion in terms of failure index (FI) is used for laminate strength evaluation. Besides, laminate strain is also commonly concerned by designers to estimate the margin of safety considering impact damage and fracture.

When comes to flutter analysis stage, FE method is also commonly applied nowadays. Unsteady aerodynamic force can be calculated by the subsonic Doublet-Lattice theory [30]. The aerodynamic and structural models are connected by 'surface spline' interpolation method. For solving the eigen value of flutter equation, PK-method is selected because it is more suitable for the following optimization.

3.4.2 Optimization

Optimization is the most challenging part of this research, because the optimal solution of an aircraft structure design should be the best compromise taking all

relevant requirements into account. These design requirements are treated as the multiple constraints during optimization.

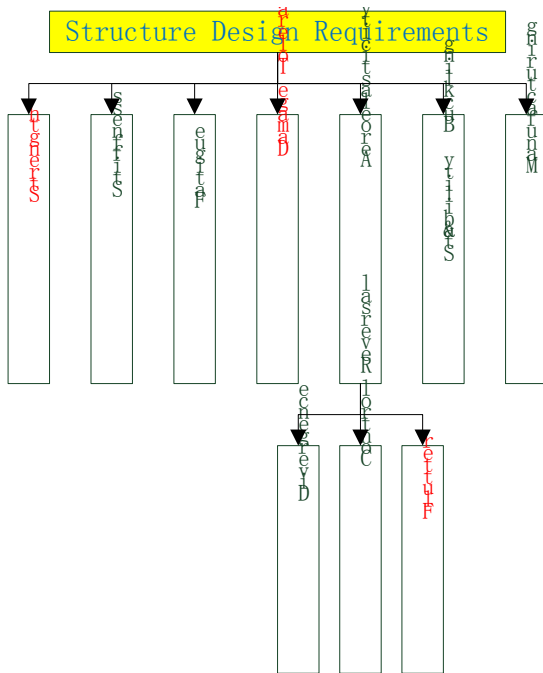


Figure 3-1 Structure Design Requirements

However, meeting all requirements at the same time significantly increases the complexity of the problem. For the purpose of simplifying the design and optimization, some requirements such as strength, damage tolerance and flutter are chosen as the multiple constraints in this example. The reason is that these requirements are always considered to be important by structure designers and can generally cover other constraints under most situations. During the optimization process of this research, both static strength and dynamic aeroelastic stability analysis were performed simultaneously. Consequently, a multidisciplinary optimization with multi-constraint was carried out in order to achieve the objective of minimum structure weight. Sensitivity of FI, maximum strain, and flutter speed to optimized lay-ups has been considered when employing GD optimization method. The laminated wing skin thicknesses are chosen as the design variables because of their effective influences to the wing structure strength, stiffness and structure weight.

3.4.3 Design Tools

In the early days, finite element models were built manually. Because of the huge amount of data to be handled, manual model-building is tedious, time-consuming, costly, and error-prone. To overcome these deficiencies, pre-processors or 3-D mesh graphics programme from CAD/CAE (Computer-Aided Design and Computer-Aided Engineering) system were developed to aid in model building. One of the earliest FEM programs and probably the most well-known is NASTRAN (NASA STRuctural ANalysis), developed by NASA in the mid-1960s to handle the analysis of missiles and aircraft structures. A pre-processor software for NASTRAN is called PATRAN and it makes the analysis of large complex structure mentioned above feasible.

Nowadays, NASTRAN is becoming a well-developed analysis method and is also commonly applied in aeroelastic analysis. In NASTRAN flutter analysis module, aerodynamic and structural models are developed independently and then connected together by interpolation method.

MSC.NASTRAN is one of the most versatile FE tools and also contains a powerful multidisciplinary optimization module. For an optimization procedure to be of maximum benefit, it must be able to simultaneously take into account of all the conditions that impact the design. For this reason, the design sensitivity and optimization capability in MSC.Nastran is based on a multidisciplinary analysis capability that includes statics, normal modes, buckling, direct and modal frequency, modal transient, static aeroelastic, and flutter analyses.

By contrast, other famous FE software, such as Hyperworks, is also powerful on optimization. But it cannot involve aeroelastic analysis. Consequently, the optimization work of this research made full use of NASTRAN code which can keep the whole analysis and optimization process within one commercial package for practical application. After the definition of objective, design variables, responses and optimization constraints in MSC NASTRAN input file, the optimization module can figure out a theoretical optimum result, which

provides a better foundation compared with initial design for designers to refine structure sizes.

Table 3-1 Stage Tasks and Tools

Stages	Tasks	Outputs	Tools
Conceptual	Structure Layout Design	3D Model	CATIA
	Material Selection	Material Property	MSC. Patran
Preliminary	Initial Sizing		
	Finite Element Modelling	FE Model	
	Static Analysis	Displacement, Stress, Failure Index	MSC. Nastran
	Flutter Analysis	Critical flutter speed, Frequency, Mode of vibration	
Optimization	Optimised skin laminates		

Besides MSC.NASTRAN, the CAD software CATIA is used to generate a 3D structure layout model as the foundation of creating FE mesh in early design stage. Finally, all the tools used in this research are listed in Table 3-1 according to different tasks.

4 Derivation of Structural Design Data

4.1 Wing Geometry and Specification

FW-11 is a new flying wing morphology commercial airliner. The standard model is a middle-size (250 seats) long-range (7,500 nautical miles) passenger aircraft to meet the increasing international air traffic demand in the next 10 years in the world. Later development can be a larger-size (around 350 seats) medium-range (4,000 nautical miles) issue to meet rising domestic air traffic demand in China and Asian Pacific area. A freighter variant is also included in the family issue of FW-11. The geometry of standard model is shown in Figure 4-1 with parameters in Table 4-1.

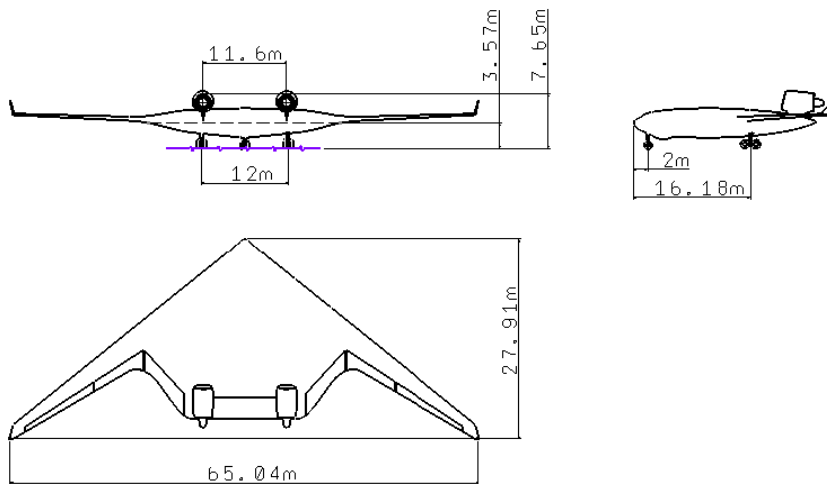


Figure 4-1 Three-view Drawing of FW-11

Table 4-1 Geometry Parameter of FW-11

Gross area	647 m ²
Wing loading	272 kg/m ²
Aspect ratio	6.33
Root chord	25.2 m
Tip chord	2 m
Taper ratio	0.11
Leading edge sweep angle	39°
Quarter chord sweep angle	34.3°

Mean aerodynamic chord	12.28 m
Dihedral angle	2 °
Central wing airfoil	NASA Langley SC Symmetric
Outer wing airfoil	NASA RC-SC2
Winglet airfoil	NACA 0012

The main specifications are listed in Table 4-2.

Table 4-2 Specification of FW-11

Seats	208(3-class), 248 (all economy)
Range(nm)	7,500
MTOW(kg)	176,469
OEW(kg)	75,044
Payload(kg)	28,686
Service Ceiling(ft)	35,000
Mach No.	0.82
Fuel capacity(kg)	72,739
Fuel/pax/nm(kg)	0.035

4.2 Load Analysis

Aircraft loads are those forces and loadings applied to the airplane structural components to establish the strength level of the complete airplane.

In terms of loads distribution, a flying wing aircraft is slightly different from the conventional wing-fuselage airliner. Flying wing is an all-lifting-surface configuration including the cabin area, which makes the aerodynamic more efficient. Meanwhile, the structure can also benefit from the relatively dispersive payload which has an effect of load-off to aerodynamic lift. However, the internal pressure applied to box type cabin area has negative influence on structure weight.

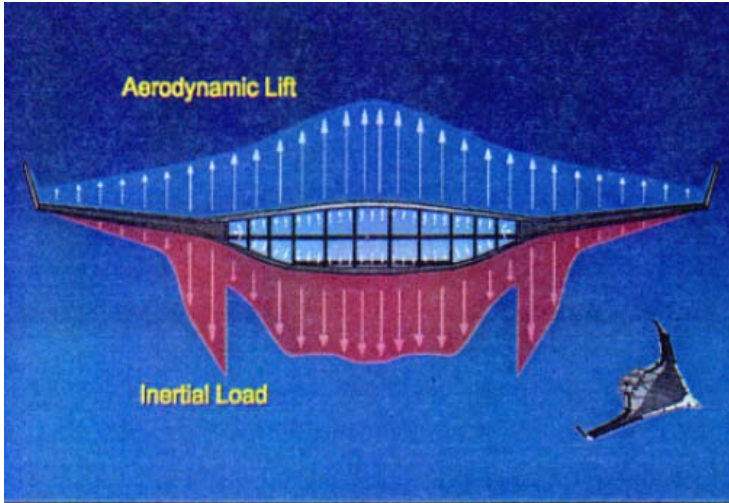
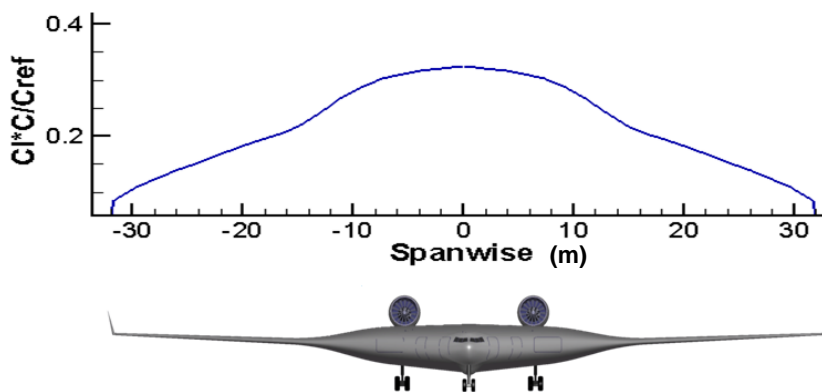


Figure 4-2 Flying Wing Aircraft Loads Condition

In conceptual design stage of FW-11, the aerodynamics in terms of lift coefficient for cruising level flight condition was calculated by aerodynamic group. The spanwise distribution taking the following form is illustrated in Figure 4-3. For inertial characteristic, the spanwise distributed mass is shown in Figure 4-4. From these data, distributed aerodynamic and inertial loads can be calculated. These distributed loads will be the fundamental for deriving shear force, bending moment and torque diagram in next step.



C_l = Lift Coefficient C = Chord Length C_{ref} = Reference Chord Length

Figure 4-3 Span-wise Lift Distribution for Level Flight

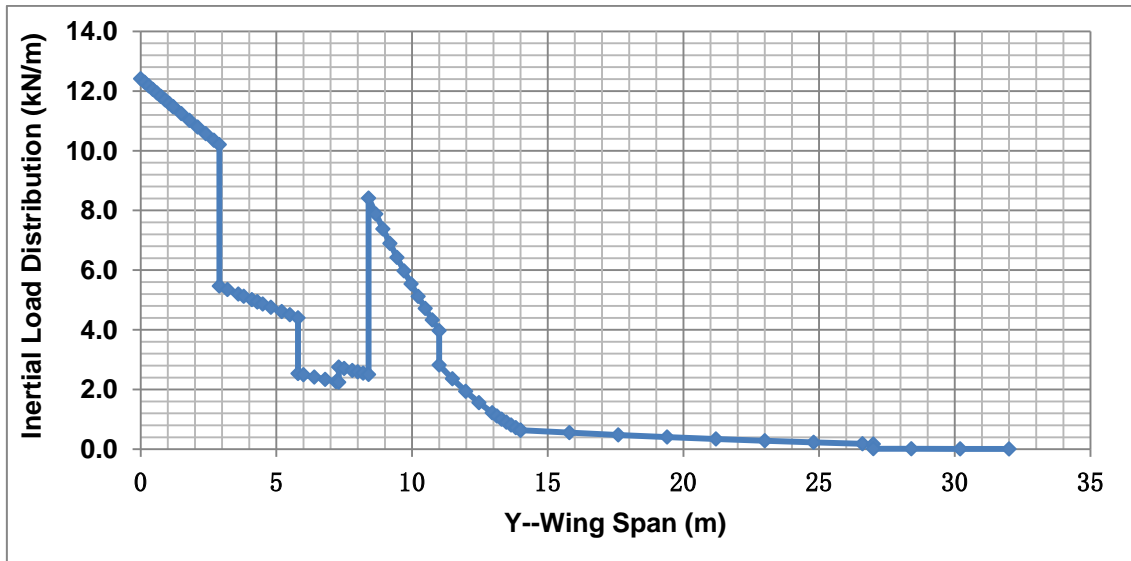


Figure 4-4 Span-wise Mass Distribution

From the loads distribution mentioned above, shear force, bending moment, and torque diagrams can be derived. The mathematical integration computing needs to be performed. This procedure is important and necessary for the following classical initial sizing calculation.

Level flight under MTOW is the most basic condition for FW-11 aircraft. The share forces caused by lifting loads and distributed mass were calculated and plotted in Figure 4-5. In normal straight and level flight the wing lift supports the weight of the airplane. Thus shear force at aircraft middle plane is equal to zero. The bending moment and torque diagrams are shown in Figure 4-6 and Figure 4-7.

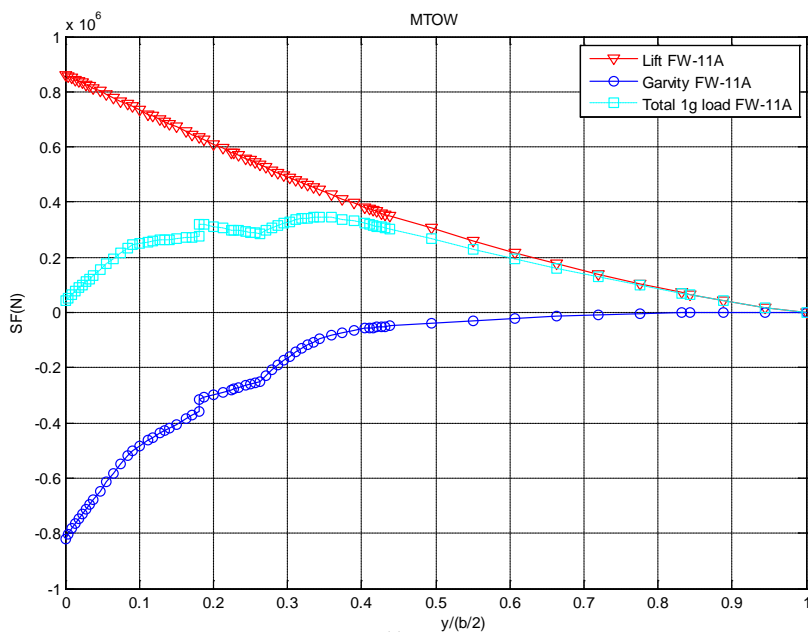


Figure 4-5 Shear Force Diagram

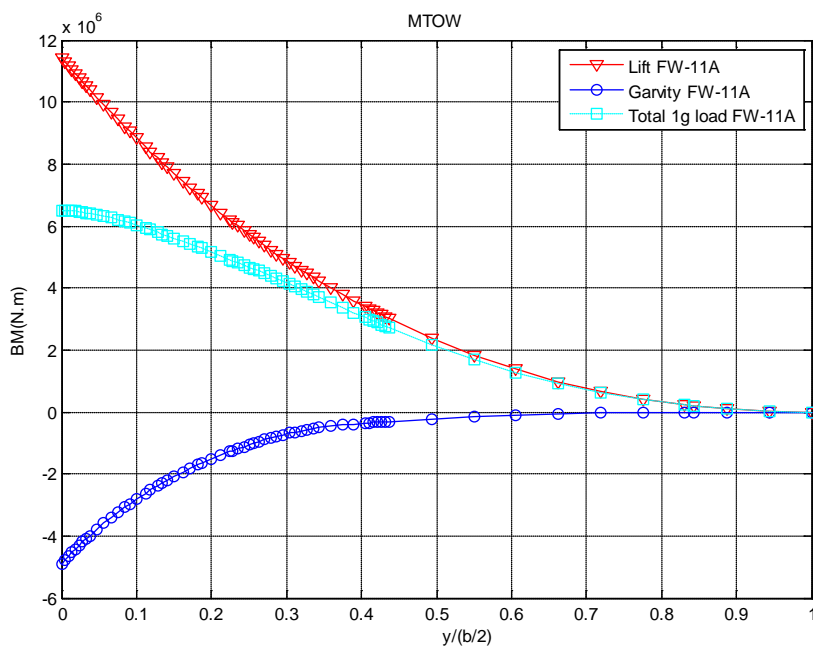


Figure 4-6 Bending Moment Diagram

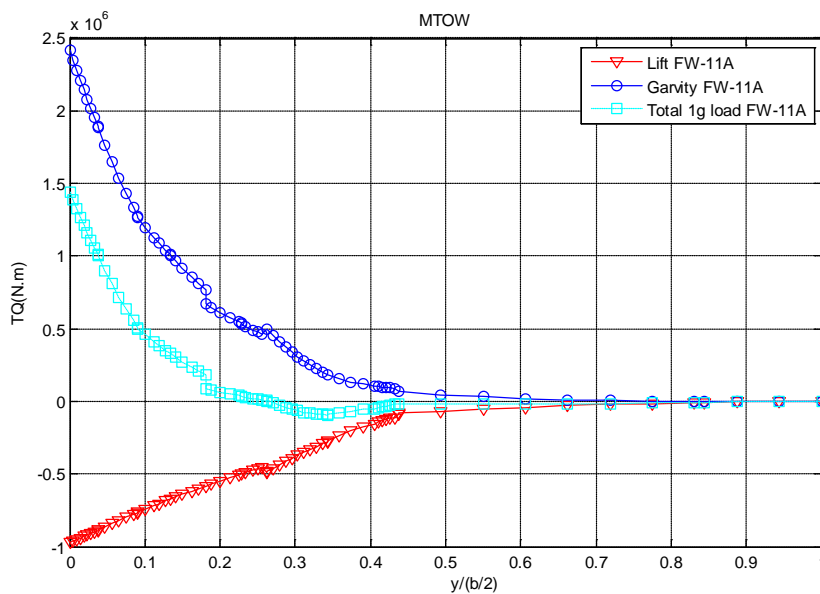


Figure 4-7 Torque Diagram

It is important to note that, these diagrams are just for 1g level flight, not the worst load case. Actually, during manoeuvres or flight through turbulent (gusty) air, however, additional loads are imposed which will increase or decrease the net loads on the airplane structure. The amount of additional load depends on the severity of the maneuvers or the turbulence, and its magnitude is measured in terms of load factor. In this FW-11 conceptual design stage, the detail loading data for other load cases is not available. But the maximum load factor for this commercial airliner was specified in the specification [37] with the value of 2.5. Consequently, the design limit load (DLL) for the following structure preliminary design was approximately obtained by using 1g condition loads multiplied by 2.5.

The design ultimate load (DUL) is the load to be carried by the structure or member without rupture or collapse and is obtained by multiplying DLL by the factor of safety of 1.5. Different from load factor, this factor is intended to cover for accuracy of load, analysis, etc. Therefore, a total factor 3.75 was adopted based on the 1g loads for the following initial sizing, FE static analysis and optimization.

4.3 Material Selection

Structure weight has always been important for aircrafts. And the use of light materials is one of the most efficient approaches to save structure weight.

Airframe designers demand strong, stiff materials at an acceptable weight and cost. Aluminium alloy has been the principal materials in airframe design for many decades. Another material that is having a major effect on aircraft design is the rapidly growing percentage of parts made of composites.

The use of composites material in a flying wing airframe is more compelling than in a conventional aircraft, especially for pressurized cabin structure. The reason is that the stresses caused by repeated pressure load on cabin structure result in fatigue problems. This is more pronounced on flying wing cabin where the structure carries the pressure loads less efficiently than a circular cross section. To achieve an adequate aircraft fatigue life, an aluminium structure would have to be heavily over designed for static loads. By contrast carbon fibre has a longer fatigue life. Thus a composite cabin is considered as an 'enabling technology' for the flying wing airliner, as the weight penalty of aluminium would negate the advantages of the new concept. In this project, CFRP sandwich panels are used in pressurized area, as the relatively thicker sandwich structure can obtain higher stiffness in bending caused by internal pressure loads.

For the outer wing structure of FW-11, the use of composite materials is also very important. Especially for the upper and lower panels of the wing box, CFRP laminates are applied taking advantage of its designable ability. The outer wing is more flexible than inner wing, and will boasts large deformation due to flight load. The large sweepback angle makes the aeroelastic characteristic worse. CFRP is usually tougher than aluminium, which means a high stiffness of the wing box can get more easily. In addition, by laminate layups design, different material properties can be achieved suitable to different load conditions. The designers can even make full use of the bending-torsion

coupling effect of the laminate to improve aeroelastic behaviour. All these advantages above play an important role in aeroelastic tailoring technique in modern aircraft design. In this project, a high modulus carbon/epoxy composite, T300/N5208 was chosen as the material of upper and lower skins for outer wing.

Table 4-3 Material Properties of T300/N5208

Notations	Description	Values
E_1	Longitude Young's Modulus, GPa	181
E_2	Transverse Young's Modulus, GPa	10.3
G_{12}	Shear Modulus, GPa	7.17
ν_{12}	Poisson's Ratio	0.28
X_t	Longitudinal Tensile Strength, MPa	1500
X_c	Longitudinal Compressive strength, MPa	1500
Y_t	Transverse Tensile Strength, MPa	40
Y_c	Transverse Compressive Strength, MPa	246
S	Shear Strength, MPa	68
ρ	Density, kg/m ³	1,600
t	Laminate thickness, mm	0.125

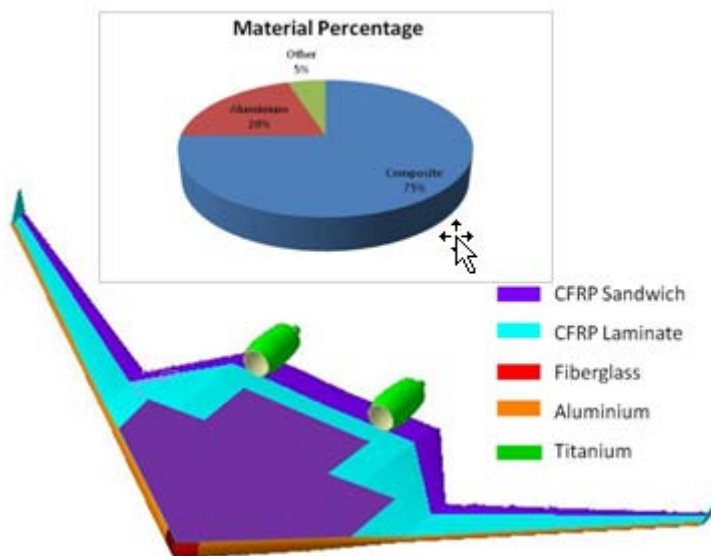


Figure 4-8 FW-11 Material Breakdown

Besides CFRP, a small percentage of other materials are used for specific components. Another type of composite, fibreglass, is applied on the nose of the aircraft in order to allow radar waves pass through. Titanium is the major material for engine pylons. It is important to point out that composite material is not suitable for leading edge area where has a high possibility of bird strike because of its vulnerability to impact damage. Hence, aluminium is the first choice for leading edge skins.

Consequently, composite materials give great promise for lighter airframes with longer life and better fatigue resistance. Such weight savings will result in greater payload for a given take-off weight, and hence greater fuel economy.

5 Structural Layout Design

5.1 General View

After the basic wing shape has been decided, a preliminary layout of the flying wing aircraft structure has been designed to carry loads during flight and upon landing. The whole FW-11 structure is mainly divided into inner wing and outer wing. As illustrated in Figure 5-1, the inner wing was generally composed of Cabin, Cargo Compartment, Flight Deck, and Engine Pylon. All the payloads are held in inner wing. The outer wing is a clean lifting surface with control surfaces on trailing edge. They are assembled together at the position of Initial Breakdown Interface which is located just outside of the pressure area.

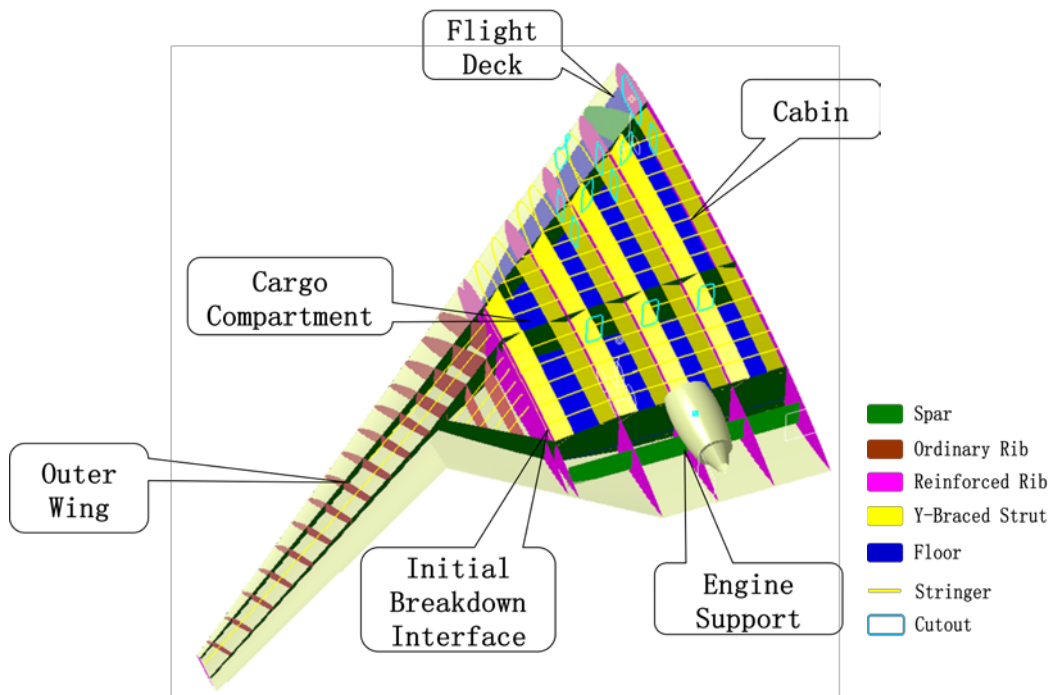


Figure 5-1 Main Structure Layout

5.2 Inner Wing Structure Concept

Like a conventional wing, the primary structure of the inner wing is built up with spars, stringers, ribs and covers which form a wing box to withstand

aerodynamic loads. The front, middle and rear spars are located at a suitable chord-wise station to give an adequate volume for cabin layout design under the certain wing shape. At last, the front spar is located at 14% wing chord, middle spar at 50% and rear spar at 80%. The transverse reinforced ribs divide the inner wing into several bays for cabin or cargo compartments. The reinforced rib distance is determined by seat arrangement and size of cargo container. A large value of 2.9m is finally adopted as shown in Figure 5-2.

However, the structure of pressurized cabin area for FW-11 is more complex than ordinary wing. The cabin structure design is one of the biggest challenges in this flying wing airliner project. Compared with traditional cylindrical fuselage, flying wing aircraft has a non-cylindrical box type cabin area which is not suitable to be a pressurized vessel. The stress level would be extremely high because the internal pressure mainly causes bending stress rather than membrane stress.

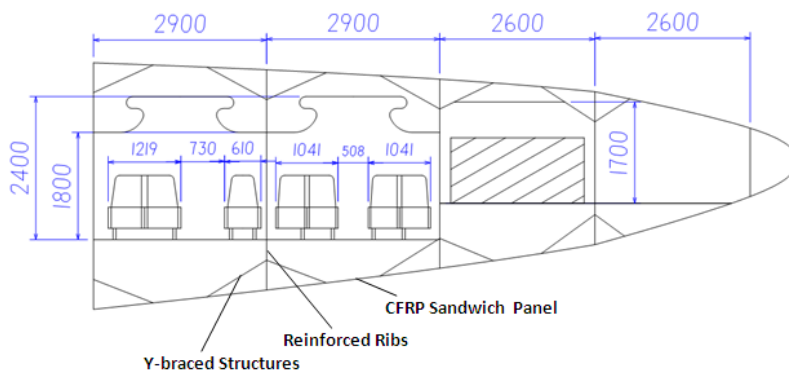


Figure 5-2 Inner Wing Structure Layout

The special design for this challenge is the use of Y-braced structures recommended by Mukhopadhyay V [31] applied in a blended-wing-body (BWB) aircraft. Y-braced structures are chord-wise members attached between ribs and covers (shown in Figure 5-2). It is important to point out that, the Y-braced structure in pressurized area had two functions. One is to serve as the pressure boundary to reduce the bending stress caused by the cabin pressure, i.e. to make each bay more close to a cylindrical vessel. On the other hand, the Y-

braced structures also help the reinforced ribs to support the top and bottom skin panels, taking the same role as ordinary ribs, due to the large reinforced rib distance. The integrated CFRP sandwich structure is applied for top and bottom panels to increase the ability of resisting out-plane bending caused by internal pressure load.

5.3 Outer Wing Structural Layout

Compared with the inner wing, the outer wing has a much more flexible structure due to its high-aspect-ratio platform feature and small wing depth. Besides, the large sweepback aggravated the bending and torsion coupling effect. Therefore, more attention should be paid on bending and torsion stiffness when design the outer wing structure. In this thesis, the outer wing main box was chosen as the example for preliminary design, analysis and optimization. And dynamic aeroelastic stability was calculated to cover the wing stiffness.

The outer wing box is mainly a two-spar structure. The locations of the front spar and rear spar are determined by the inner wing spar locations and the size of trailing edge control surfaces. The front spar is kept consistent with the inner wing front spar at outer wing root, and at wing tip it is located at 14% tip chord. The rear spar is kept consistent with the inner wing middle spar and located at 60% chord which is a proper station to support the control surfaces. Another tilt short spar is added in kink area connecting rear spars of both inner and outer wing to share part of loads. The longitudinal spars are in charge of passing all shear force and part of bending moment.

The upper and lower wing covers should be utilized to a large extent in carrying wing bending. That is because the high torsional rigidity is required for this flexible large sweepback wing. Thus the covers need large percentage of torsional material to achieve this rigidity. It is the same material that can as well be used for both primary bending and torsion. The wing covers are designed as composite skin-stringer panels. The longitudinal stringers are needed to

increase the buckling stability. And a typical pitch of 200mm is adopted according to other large aircraft statistics in Niu's handbook [26].

After wing spars are located, the wing ribs can be arranged. In consideration of the direction, the ribs are finally arranged normal to the rear spar. Such layout has advantages in supporting control surfaces, manufacture, and weight saving. The rib spacing is determined from panel-size considerations. Generally, it is a variable value with the depth of the wing box and has the maximum spacing at the inboard end. The rib spacing of this outer wing for large airliner is 800mm recommended by Niu M [26] as well.

Finally, the main elements of the outer wing structure have now been located as illustrated in Figure 5-3.

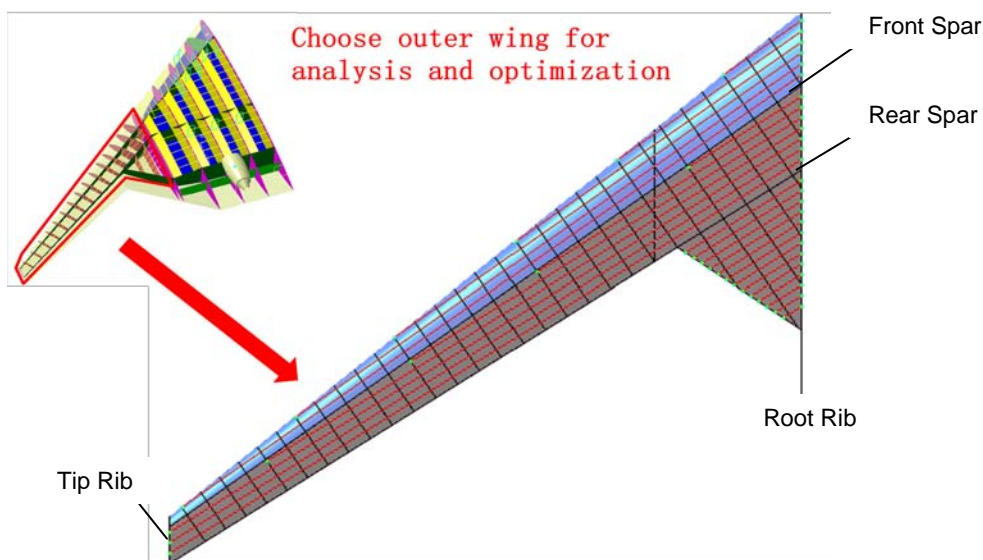


Figure 5-3 Outer Wing Structure Layout

6 Classical Initial Sizing

After the outer wing structural layout was arranged, the structural member size is mainly dependent upon the load level and material property. Structure loads can be derived directly from shear force, bending moment and torque diagram (Figure 4-5, Figure 4-6 and Figure 4-7). Although material property of composite laminate can be obtained by numerical program, in this chapter, classical method using hand estimation was adopted firstly.

6.1 Composite Material Property Estimation

Apart from potentially high material properties an advantage of fibre-reinforced composite is the ability to tailor the properties to meet a given set of requirements. However, this directional nature also makes the estimation of composite material property more complex than isotropic metallic material.

For this preliminary design stage, the most important material properties needed to perform structure member initial sizing work include stiffness and allowable strength for a certain laminate construction. Stiffness mainly consists of elastic modulus (E) and shear modulus (G). The single-layer material has been selected previously and the basic properties are listed in Table 4-3. However, for a certain laminate construction, the plies in each direction of the laminate make some contribution to the load carrying capacity in any given direction. And therefore the overall stiffness and strength is a complex function of the number and direction of the plies as well as the matrix properties.

Denis Howe's classical method is to limit the choice of fibre orientations to four specific directions, namely a datum at 0° , defined by the primary loading, together with 90° and $\pm 45^\circ$ to simplify the laminate property estimation. Then a simple method, called '10 per cent rule' proposed by Hart-Smith [28], is used to make approximate stiffness calculation for the directional interactions. This rule is based on the assumption that relative to the reference 0° direction each 90° , $+45^\circ$ and -45° ply contributes 10 per cent of its directional strength or stiffness.

In order to simplify the hand calculation work for design and analysis, a quasi-isotropic lay-up laminate construction has been used for the initial design stage of this example, which means a laminate has an equal number of fibres in each of the four directions. According '10 per cent rule', 75% layers in all of 90°, +45° and -45° directions contribute 7.5% of its directional stiffness. Thus the equivalent tensile stiffness can be estimated as 32.5% E_{x0} , where E_{x0} is the directional modulus of elasticity. Shear stiffness is calculated by taking 50 per cent of the directional stiffness of a complementary lay-up defined as one having the sum of the 0° and 90° disposed equally in the $\pm 45^\circ$ directions. Application of the method to shear stiffness yields a value of 0.122 E_{x0} for the quasi-isotropic lay-up. [27]

$$E = 32.5\% * E_{x0} = 0.325 * 181GPa = 58.8GPa \quad (6-1)$$

$$G = 12.2\% * E_{x0} = 0.122 * 181GPa = 22.1GPa \quad (6-2)$$

For allowable strength estimation, Howe recommended that ultimate direct allowable tensile stress can be calculated by using the elastic moduli with suggested allowable strain 0.004 [27].

$$\sigma_b = E * \varepsilon = 58.8GPa * 0.004 = 235MPa \quad (6-3)$$

However, allowable compression may depend upon the buckling characteristics of the component. Tetlow [32] proposes the following for overall buckling:

$$\sigma_b = 0.725 F_B \left\{ (E_{x0})^2 Z_0 \right\}^{1/4} \left\{ P / (wL) \right\}^{1/2} \quad (6-4)$$

Where F_B is buckling efficiency factor dependent on panel construction

E_{x0} is directional modulus of elasticity

Z_0 value is a function of the lay-up, determined in Tetlow's chart

P is the effective end load which coincides with the maximum direct stress

w is the width of the component perpendicular to the bending axis
 L is the spacing along the axis of the beam of the local supports

For allowable shear stress, following value is suggested for initial calculations for a quasi-isotropic lay-up.

$$\sigma_s = 200MPa \quad (6-5)$$

6.2 Structure Member Initial Sizing

Classical initial sizing technique for a wing structure is based on direct use of the shear force, bending moment, and torque diagrams.

First of all, these basic loads should be converted to local forces applied to specific structure members according to the wing box dimensions at several typical sections. The cross-section dimensions at wing root, tip, and kink position are shown in Figure 6-1.

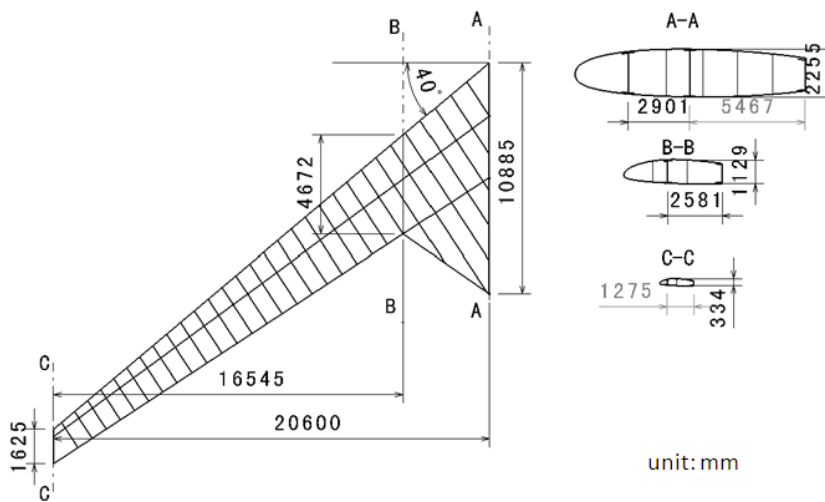


Figure 6-1 Dimensions of Wing Structural Box

6.2.1 Spar Webs

The front and rear spar web reactions due to the ultimate vertical shear loads are calculated as below:

$$F_1 = Vh_1^2 / (h_1^2 + h_2^2) \quad (6-6)$$

$$F_2 = Vh_2^2 / (h_1^2 + h_2^2) \quad (6-7)$$

Where V is the applied ultimate vertical shear load; h_1 and h_2 are the depths of the front and rear spars respectively.

As a result, the shear flow in the spar webs can be calculated by:

$$q_1 = F_1 / h_1 \quad (6-8)$$

$$q_2 = F_2 / h_2 \quad (6-9)$$

However, the evaluation of thickness of spar web should also add the effect of torsion loads. The corresponding shear flow in the covers and webs is approximately:

$$Q_T = T / 2A \quad (6-10)$$

Where T is the magnitude of the ultimate applied torsion loads; A is the enclosed area.

The net shear flow in the webs is then given by:

$$Q_1 = q_1 + Q_T \quad (6-11)$$

$$Q_2 = q_2 + Q_T \quad (6-12)$$

Finally, the thickness of spar webs are obtained from

$$t = Q / \sigma_s \quad (6-13)$$

6.2.2 Composite Skin

The effective direct loads P in the top and bottom surfaces required to react the appropriate ultimate bending moment M at each section is:

$$P = M / h \quad (6-14)$$

Where h is the mean depth of the primary structural box.

Then the cross-section area required to meet this direct loads is figured out:

$$A_b = P / \sigma_b = M / (h\sigma_b) \quad (6-15)$$

An equivalent thickness including skin, stringers and spar caps can be derived from this cross-section area:

$$t_e = A_b / w = M / (hw\sigma_b) \quad (6-16)$$

Where w is the width of the box.

Typically the effective thickness due to the stringers is between 50 and 100 per cent of that of the skin, depending upon the form of construction and the load intensity. In this example, a lower value was chosen, and the actual skin thickness needed in the bending case is approximately:

$$t_b = 0.65M / (hw\sigma_b) \quad (6-17)$$

As mentioned above, quasi-isotropic laminate construction was selected to simplify the calculation. And all the laminated structures were designed symmetrical and balanced due to manufacturing consideration.

Considering a typical wing box which is tapered from wing root to wing tip, it is optimum to have the thickness of material reduced gradually coinciding with the load condition. In initial structure design, the outer wing was divided into nine zones (zone 0~8, shown in Figure 6-2) which were defined with the positions of the ribs as the boundary. At different design zone position, the wing box cross-

section dimensions were measured in CATIA model. Then initial sizing calculation introduced above was implemented separately.

Finally, the initial sizes of CFRP layup skin in the nine regions are listed in the Table 6-1.

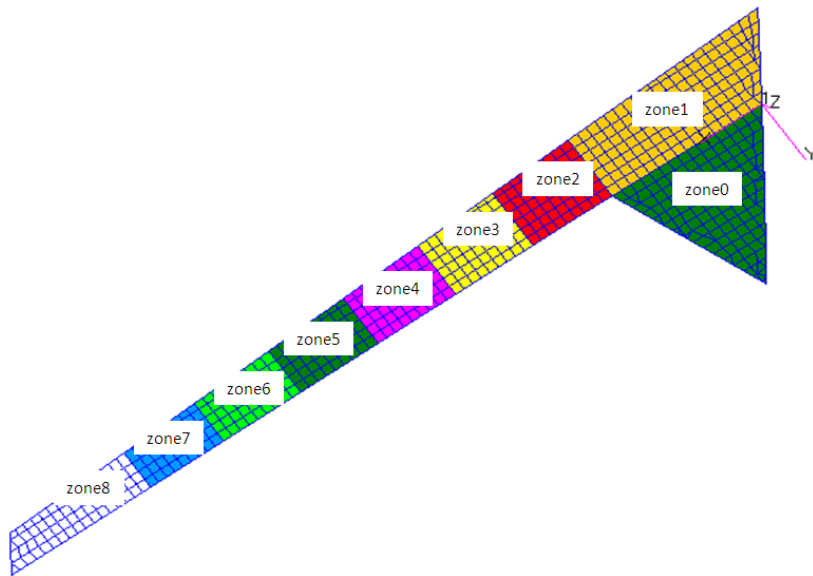


Figure 6-2 Design Zones of the Outer Wing

Table 6-1 Skin Laminate Thickness in Initial Design

Components	Section	T(mm)	Ply Percentage(%)		
			0	±45	90
Top Skin	zone0	8	25%	50%	25%
	zone1	12	25%	50%	25%
	zone2	14	25%	50%	25%
	zone3	12	25%	50%	25%
	zone4	10	25%	50%	25%
	zone5	8	25%	50%	25%
	zone6	6	25%	50%	25%
	zone7	4	25%	50%	25%
	zone8	2	25%	50%	25%
Bottom Skin	zone0	8	25%	50%	25%
	zone1	12	25%	50%	25%
	zone2	14	25%	50%	25%
	zone3	12	25%	50%	25%
	zone4	10	25%	50%	25%
	zone5	8	25%	50%	25%
	zone6	6	25%	50%	25%
	zone7	4	25%	50%	25%
	zone8	2	25%	50%	25%

7 Finite Element Approach Estimation

7.1 Static Analysis

7.1.1 FE Structure Modelling

Based on the result of structure initial sizing, the first step of the numerical analysis is to build a finite element model to simulate the real structure. However, this work for a large wing structure is still a challenging and time-consuming work. The FE structure model will be the basis of the following optimization as well.

As the pre-process of analysis, a standard FE modelling work consists of two steps: meshing and property definition.

Meshing a large complex wing structure by hand is a time-consuming job. 'Advanced meshing tool' in CAITA software was used to get an ideal result quickly (Figure 7-1). It is also very easy and useful to keep the link with CATIA structure layout model. Then the FE grids and elements were imported into MSC.PATRAN by using standard format input file for the remaining pre-process.

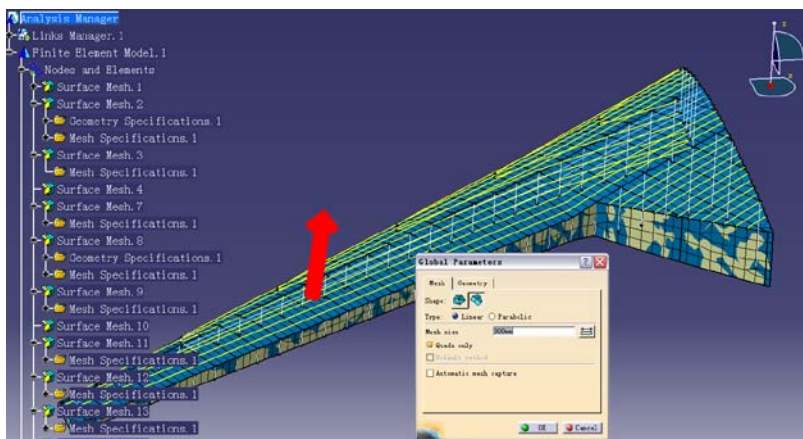


Figure 7-1 Advanced Meshing in CATIA

In this structure FE model, the skins and the webs of spars and ribs were modelled as shell elements which were mainly composed of CQUAD4 elements.

A small amount of CTRIA3 elements were used for transition in some area where structure size changed dramatically. The stringers, spar caps, spar stiffeners and rib flanges were simplified to rod model using CROD elements which share the same nodes with shell elements. Finally, the type and quantity of the whole finite elements are listed in Table 7-1.

Table 7-1 Finite Element Statistics

Element Type	Quantity
Nodes	3,349
CQUAD4	3,784
CTRIA3	200
CROD	2025

In property definition of the composite structure, the skin panel and the internal substructure of the wing box were treated differently. The following analysis and optimization will focus on the upper and lower skin panels because they make great influence to the strength, stiffness and structure weight of the wing box. Therefore, they were modelled as composite laminate on property definition, which will make the stress, strain and FI calculation for each lamina possible. Figure 7-2 shows the laminate modelling of composite skin for one of the design sections in Patran. It can be seen that the laminated skin was designed symmetrically, and the half layers were defined. The 'T300/N5208' material properties were input according to the values listed in Table 4-3.

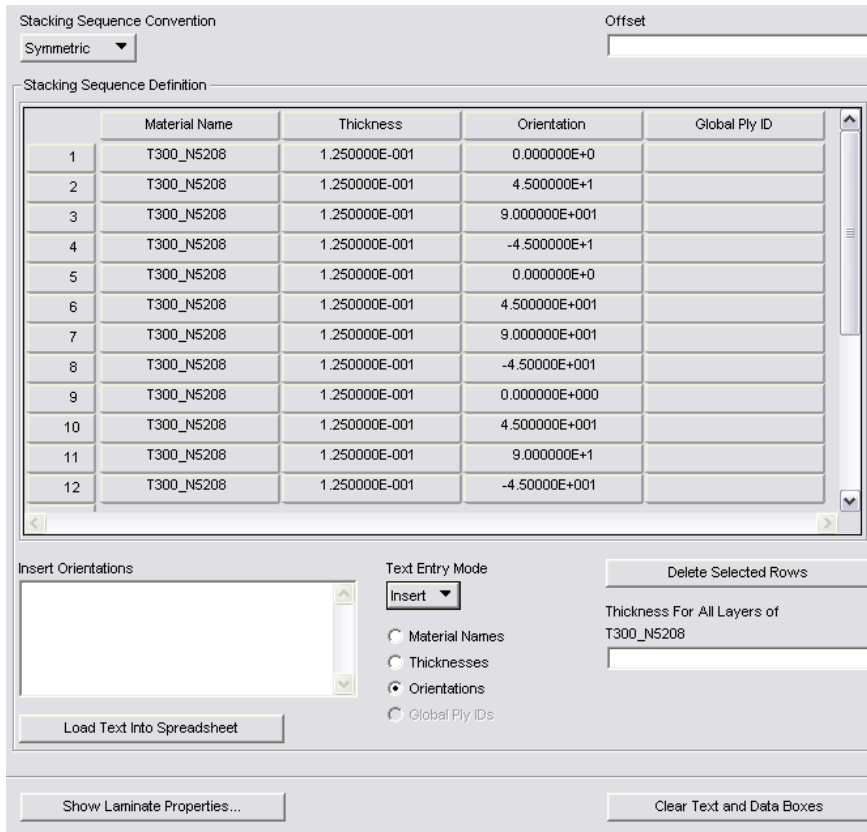


Figure 7-2 Composite Laminate Modelling in Patran

By contrast, equivalent engineering elastic constants were utilized for the internal substructure with the purpose of simplification. This treatment can get the same strain level for each component. The equivalent E values can be easily calculated by using a FORTRAN programme called “ABCMXS.exe” provided by Guo S [33]. In this research, the substructures were designed as quasi-isotropic symmetric laminates with T300/N5208 lamina. From the results of the equivalent E value calculation in membrane (in-plane) loading system, E_x and E_y are the same. Thus they were finally treated as equivalent isotropic material in NASTRAN having the similar value with aluminium alloy.

Table 7-2 Calculated Equivalent Elastic Constants

	E_x (GPa)	E_y (GPa)	G_{xy} (GPa)	ν_{xy}
MEMBRANE:	69.7	69.7	26.9	0.296

7.1.2 Distributed Loads Definition

As stated in initial sizing phase, the classical method for wing structure design is based on the use of the shear force, bending moment, and torque diagrams calculated from load distribution. However, when a finite element approach is used it is necessary to use distributed loads directly since the analysis effectively performs the integrations.

The lift and inertial spanwise distribution for steady level flight is illustrated by Figure 4-3 and Figure 4-4. They were idealized as sets of point loads applied at the nodes of the structure elements. Such procedure can conveniently be achieved by the use of the pre-processor PATRAN before the actual finite element analysis. A scale factor 3.75 was then defined in order to impose load factor 2.5 and safe factor 1.5 to get the approximate design ultimate loads. The whole outer wing was clamped on wing root. The final numerical model for static analysis is shown in Figure 7-3.

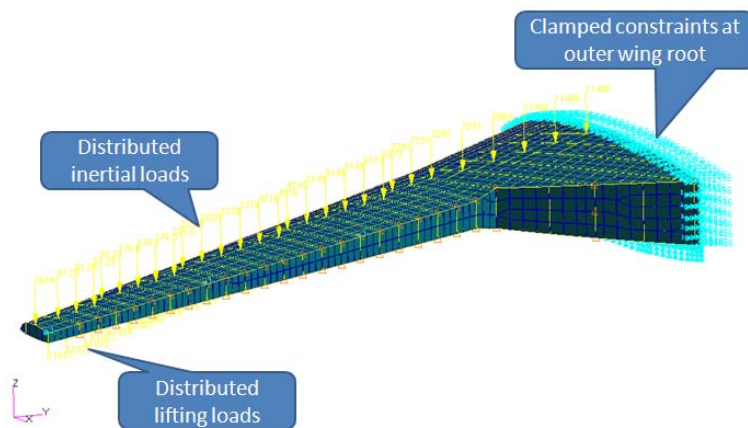


Figure 7-3 Numerical Model for Static Analysis

Based on the FE model, static strength analysis was conducted. Measured from this numerical model, the structure mass of the outer wing main box is 7,466kg.

7.1.3 Static Analysis Results

After FE modelling, the static analysis was submitted to NASTRAN solver. Based on the initial design of the wing structure, the results under ultimate load were obtained.

From the displacement result as shown in Figure 7-4, the maximum wing tip deformation is 1.18m which is a normal value for a high-aspect-ratio flexible wing.

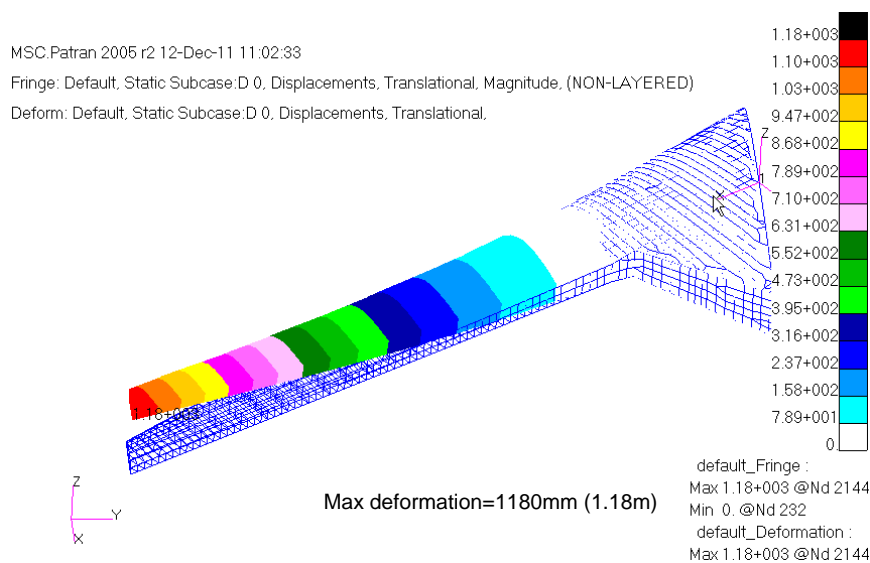


Figure 7-4 Initial Deformation Result

The primary objective of the structural designer is to achieve the maximum possible safety margin and achieve a “reasonable” lifetime of the aircraft structure. [34] This research focused on the top and bottom laminated skins. First of all, laminated skin strength usually in terms of FI was evaluated. As can be seen from Figure 7-5, the maximum FI is 0.76. Judging by Tsai-Wu criterion expressed in Equation (3-3), ply failure would not occur because FI is far below 1.0.

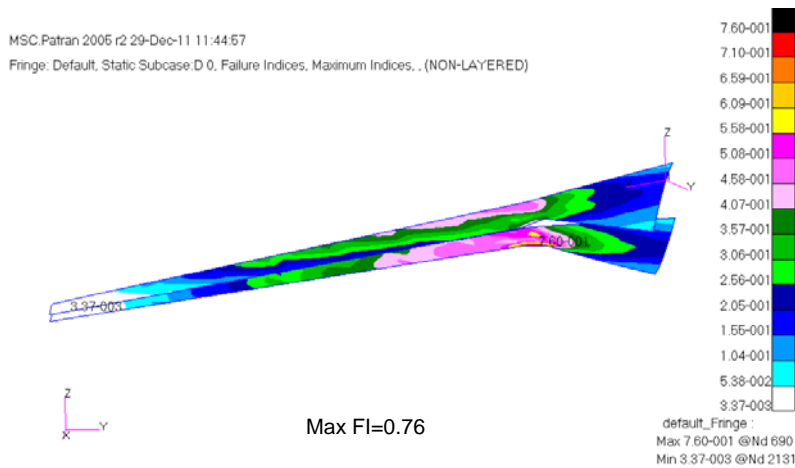
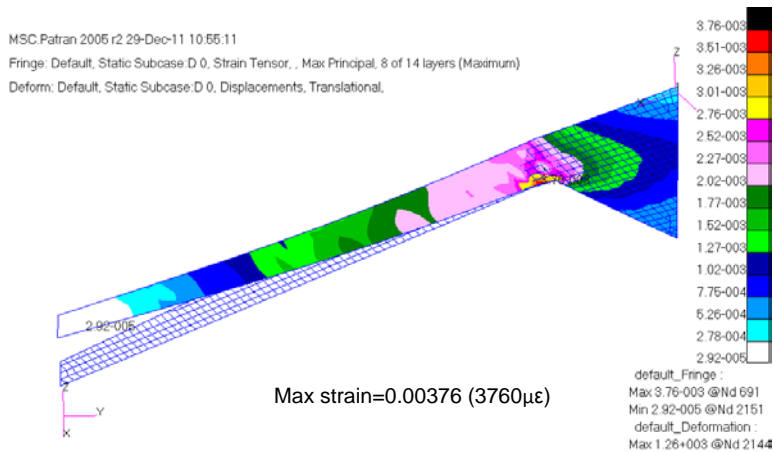


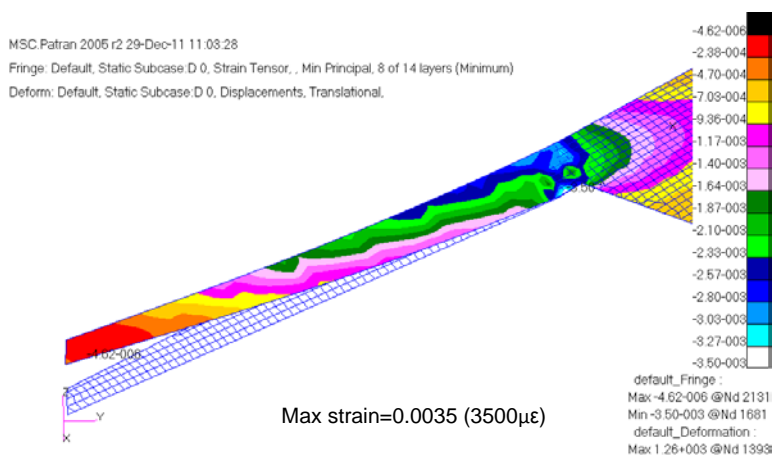
Figure 7-5 Initial FI Result of Laminated Skin

However, one of the major differences in composite analysis, as opposed to metal, is that strain is the major concern and not stress. In this example, principal strain was calculated by NASTRAN.

It is important to note that different strain item should be concerned for top and bottom skin. The bottom skin of the wing box under this ultimate load resists tensile force. Maximum principal strain should be chosen. As shown in Figure 7-6(a), the maximum value is 0.00376 (3760 $\mu\epsilon$). On the other hand, the top skin reacts compression so that minimum principal strain with minus value should be concerned. The maximum absolute value is 0.0035 (3500 $\mu\epsilon$) illustrated in Figure 7-6(b). They both occurred in the kink area of the wing where stress concentration is caused by the geometric change.



(a) Bottom Skin



(b) Top Skin

Figure 7-6 Initial Strain Result of Laminated Skin

For margin of safety analysis, a strain allowable value should be given for comparison with actual strain level. In practice, actual strain level values for composite structures of an aircraft are typically shown in Figure 7-7. It can be seen that the strain level will be very high to at least 5000 $\mu\epsilon$ in hole or defect area due to the stress concentration. In the design of large structures, one of the basic ground rules is to establish the ultimate gross area cut-off strain when designing in tension and compression-critical areas. In the application of composite material to structures, the allowable levels are low because it

automatically covers many design considerations. These considerations include tolerance for impact damage, flaw growth resistance, stress concentration associated with cutouts, reduced strength in hot/wet conditions [8]. In this example, it is set at 0.004 (4000 $\mu\epsilon$) for general area under design ultimate loads. This value of limiting strain will also be an important constraint for the following optimization.

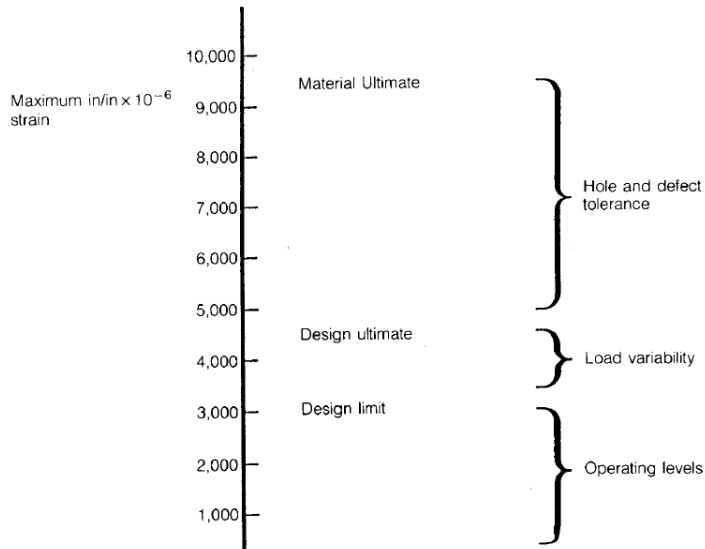


Figure 7-7 Typical Strain Level for CFRP [8]

For the internal substructure, equivalent isotropic elastic constant was used for all composite components so that lamina failure analysis cannot be performed. But the strain level can still be obtained (see Figure 7-8) for validation.

The further work in detail design stage should also include establishing composite laminate material properties for all the internal substructures. And the laminate failure analysis will also be performed.

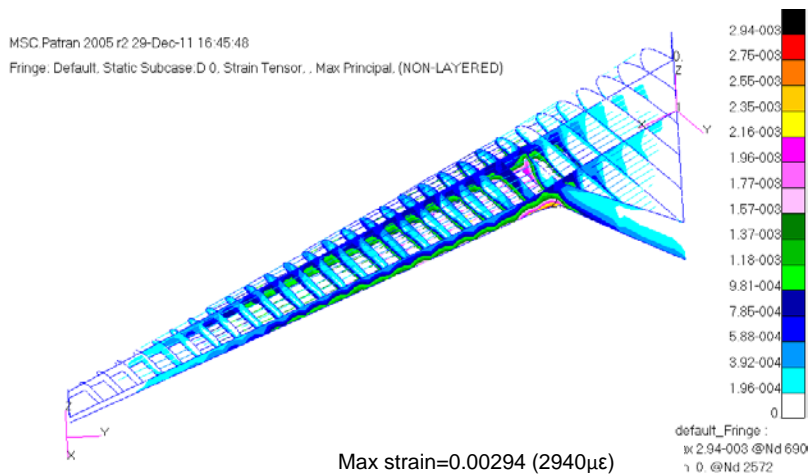


Figure 7-8 Initial Strain Result of Substructure

From the static analysis results, the accuracy of the FE approach can be verified by hand calculation. The conclusion can also be drawn that the initial design using Denis Howe’s method is reasonable but conservative, and the FE model can be used as the fundamental of optimization.

7.2 Aeroelastic Analysis

7.2.1 Modelling for Dynamic Analysis

In the modelling for dynamic and aeroelastic analysis, two types of modifications should be carried out based on the FE model for static analysis.

The first modification is to add mass data required by dynamic analysis. In fact, mass distribution also plays an important role in dynamic behaviour besides structure stiffness. In property definition phase, the material density item has been entered. Thus the wing box structure has already got the mass characteristics (amount of mass, centre of mass and moment of inertia). However, the mass of control surfaces on the trailing edge of the outer wing should not be neglected. Then the mass of outer elevator, flap, aileron and split drag rudder were distributedly applied as concentrated masses along the grids of the rear spar, as shown in Figure 7-9. Total of 0.87 tons were added to the wing main box. In practical, this mass distribution should also include the

system equipment and fuel weight. But in this example, they were ignored due to the lack of related data.

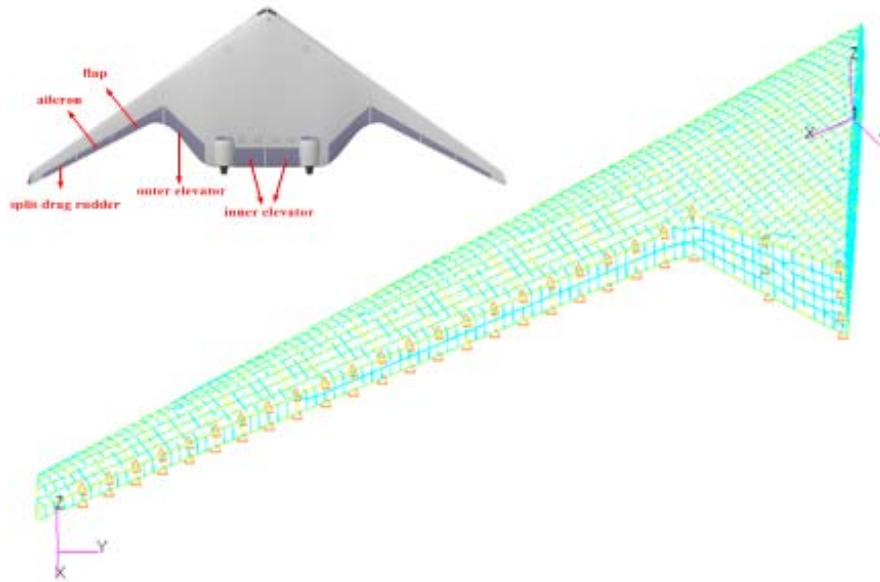
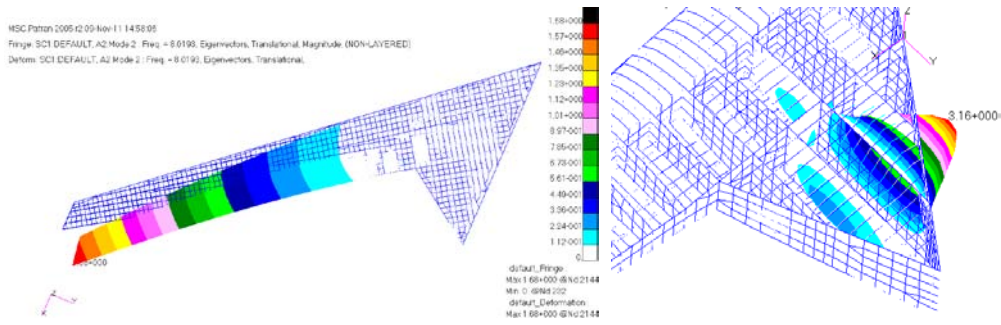


Figure 7-9 Mass of Control Surfaces

The other modification needed is to eliminate the interference modes which would not happen in real structure vibration. Before modification, there were two types of interference modes exist in this FE model: chord-wise bending mode and local modes, as shown in Figure 7-10. They were mainly caused by the model simplification commonly used in static analysis but not appropriate in dynamic analysis.



(a) Chord-wise bending mode

(b) Local modes

Figure 7-10 Interference Vibration Modes

The wing chord-wise bending stiffness should be much higher than transverse bending stiffness in real wing structure so that such bending mode should not be in such a low frequency of 8.02Hz. The simplification of connection between spar and rib webs caused this problem. The low frequency local modes happened on the webs of rib and spar is because the lack of adequate stiffeners reduced the out-plane bending resistance of the plate or the stiffeners were modelled as rod elements rather than beam elements. These modes may have great interference influence on flutter analysis result and should be eliminated.

After the modification, the first four modes of the wing are calculated and presented in Figure 7-11, which are first bending (3.63 Hz), second bending (11.89 Hz), third bending (25.48 Hz), and first torsion (32.26 Hz), respectively.

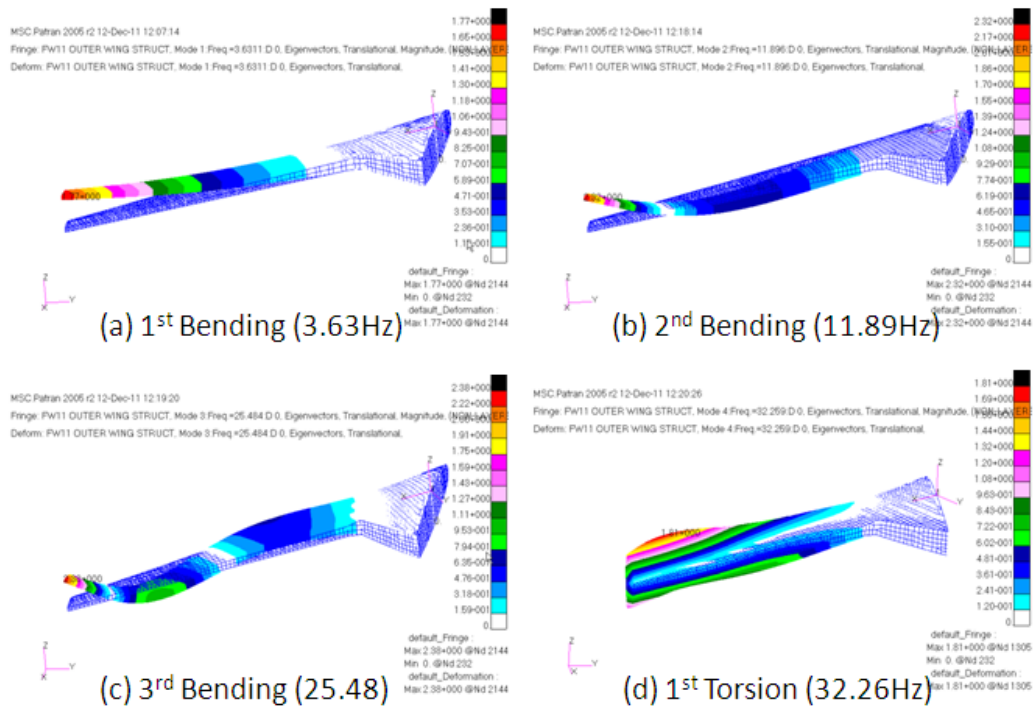


Figure 7-11 Natural Frequency Modes

7.2.2 Flutter Analysis Modelling

In order to execute flutter analysis program in NASTRAN, oscillatory aerodynamic forces, structural stiffness, and inertia properties are the essential inputs as shown in Table 7-3. The modified structure model for dynamic analysis mentioned above is used to figure out stiffness and inertia terms, while an aerodynamic model should be additionally generated to calculate the unsteady lifting forces caused by the vibration of structure in steady airflow.

Table 7-3 Inputs and Outputs for Flutter Analysis

INPUT	OUTPUT
Oscillatory Aerodynamics	Critical airspeed and frequency
Structural Stiffness	Neutrally stable oscillation at flutter speed
Inertia Properties	Oscillatory divergence above flutter speed

Aerodynamic and structural analyses are both based upon finite element approach. Aerodynamic and structural elements are developed independently. SPLINES method is then used to interpolate between aerodynamic and structural models. At last, certain aeroelastic analysis can be easily performed by choosing proper executive programmes. The whole procedure is shown in Figure 7-12.

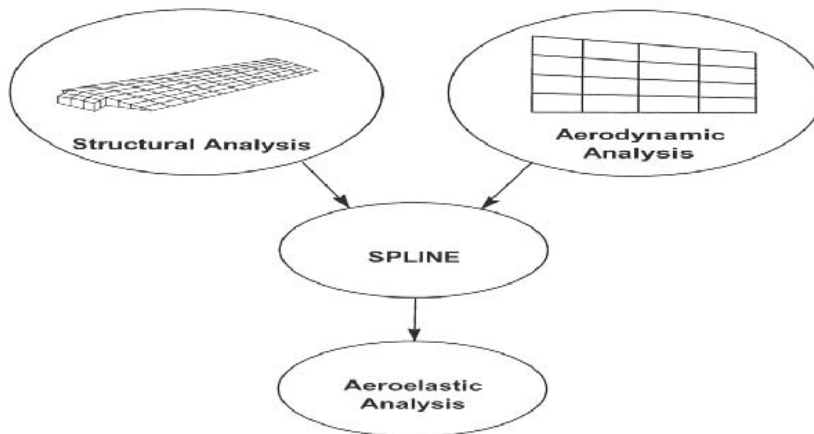


Figure 7-12 FE Method of Aeroelastic Analysis

In aerodynamic modelling, subsonic Doublet-Lattice lifting system is used. Doublet-Lattice Method (DLM) requires that all lifting surfaces are assumed to lie nearly parallel to the flow and each interfering surface is divided into small trapezoidal lifting elements 'boxes'. The boxes are arranged to form strips that are parallel to the free-stream. Fold lines and hinge lines should preferably lie on the box boundaries. For this flying wing aircraft, the lifting surface is the whole clean wing. Symmetry options are available to enable reduced problem size. The half wing is divided into three aero surfaces from the kink position. Uniform number of aero elements strategy is used when each aero surface is meshed. It can be seen from the result in Figure 7-13 that there are 7 constant of boxes in chordwise.

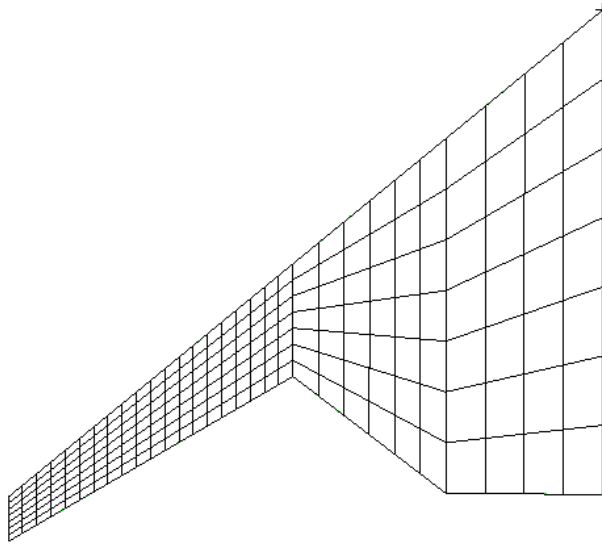


Figure 7-13 Aerodynamic Model using DLM

The structural and aerodynamic models are disjoint until the splines are used to build an interpolation matrix. This matrix is used to determine motion for the aerodynamic degrees of freedom (DOFs) based upon motion at the structural DOFs. Nastran aeroelastic analyses are performed using structural DOFs.

Two transformations for both aerodynamic forces and displacement of grids are expressed as

$$\begin{aligned} \{u\}_k &= [G_{dkG}] \{u\}_g \\ \{F\}_g &= [G_{pGk}] \{F\}_k \end{aligned} \tag{7-1}$$

where k and g represents aerodynamic and structural grid set respectively. G_{dkG} is spline matrix to convert structural displacements to aerodynamic displacements, and G_{pGk} is spline matrix to convert aerodynamic forces to structural forces. F and u are force and displacement vectors.

Several splining methods are provided in Nastran. In this example, surface splines are used to interpolate a trapezoidal array of boxes to structural grid points as shown in Figure 7-14.

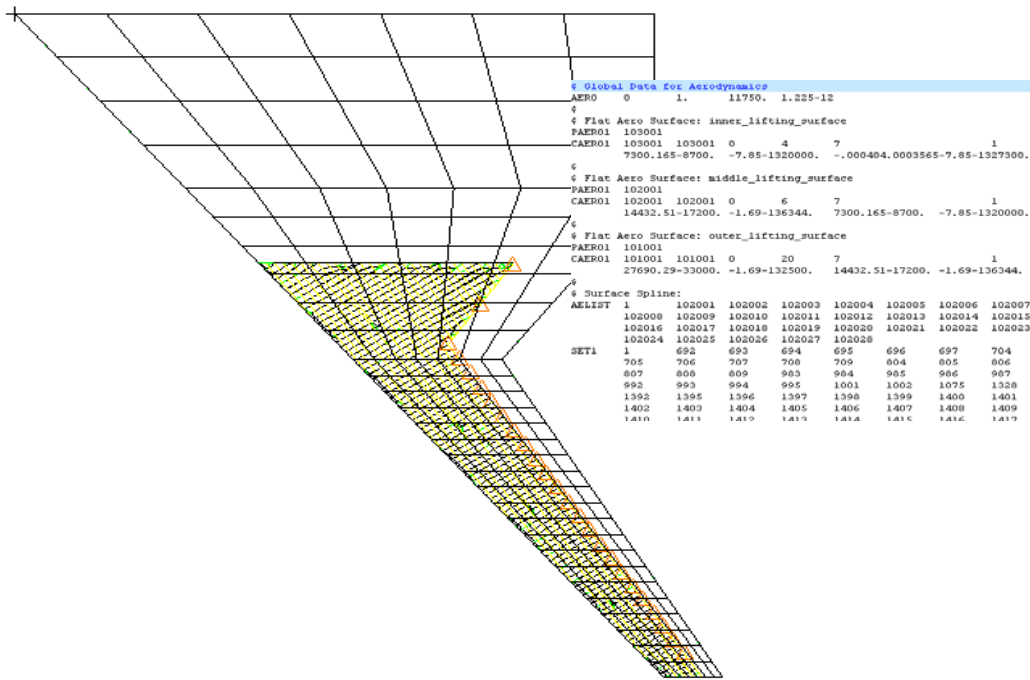


Figure 7-14 Structural-Aerodynamic Connection

The NASTR input codes for flutter modelling can be found in FW11_FLUTTER.DAT (Appendix A.3). When all the aeroelastic modelling work above is finished, the initial flutter analysis is ready to perform.

7.2.3 Flutter Analysis Results

When the aeroelastic modelling was finished, the flutter analysis was implemented using PK-method to obtain the eigen value solution of the flutter equation (Equation (3-5)).

The printed output began with a vibration analysis which gives the 10 natural frequencies of the cantilever wing. The first four modes were shown in Figure 7-11. Next, the Flutter Summaries for the first four requested flutter modes were presented, shown the damping and frequency values under specified velocities. Then the V-g and V-f curves for the PK-method were plotted and shown in Figure 7-15.

The results indicated that the first torsion vibration mode was most critical and the outer wing appeared a classical bending-torsion flutter. From the curves and the Flutter Summary together with the linear interpolation method, the lowest flutter speed at 815 m/s and frequency of 23.5 Hz was predicted respectively when the damping reaches zero.

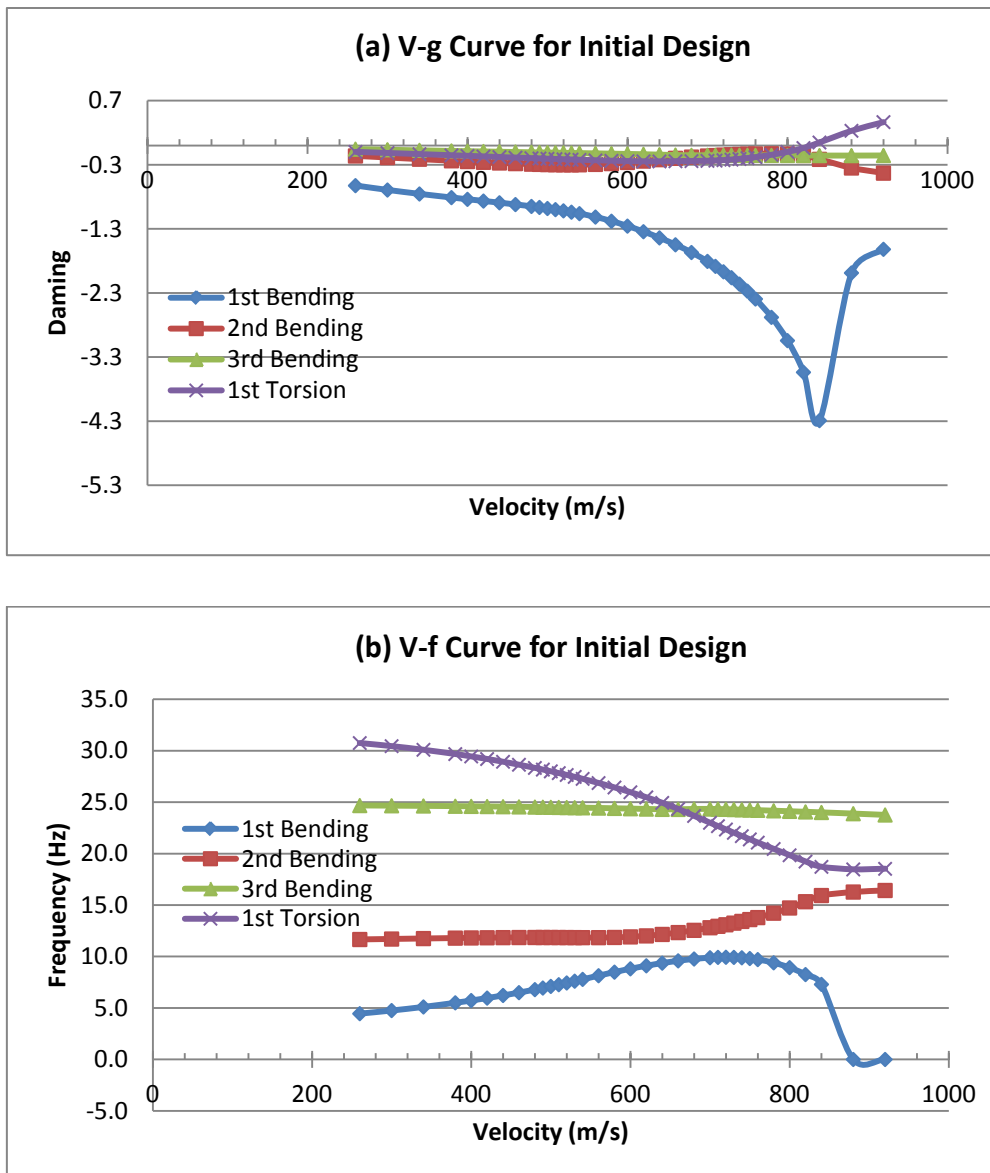


Figure 7-15 V-g and V-f Curves for Initial Design

For the aeroelastic requirement, according to CS-25.629 [35], the aeroelastic stability envelopes should not below $1.15V_D$. Design dive speed V_D is the

maximum speed for structural design providing for safe recovery from inadvertent upsets. V_D can be approximately estimated by adding a certain speed increment to design cruising speed V_C . It is recommended by Howe D [27] in terms of March number as follows.

$$M_D = M_C + 0.07 \quad (7-2)$$

From the FW-11 Specification [37], design cruising Mach number M_C is 0.82. Converted to true air speed (TAS), the design dive speed (V_D) of this aircraft is 302.6 m/s at sea level. Therefore, the critical flutter speed should not less than 348 m/s.

From the flutter analysis of initial design, the actual flutter speed is more than twice as required. Therefore it can also prove the initial design is a conservative design in dynamic aeroelastic aspect, and the structure has potential for weight saving by optimization under flutter constraint.

8 Optimization

8.1 Optimization Model Description

The initial design result of the outer wing structure was set as the start point for this optimization example. The aim was to minimize the structure weight by optimizing the thickness of laminated cover skins. All the internal substructures were kept unchanged in this research. The multidisciplinary aspect of this example involved both the static analysis under ultimate load case and the flutter analysis. The multi-constraint included Tsai-Wu FI related to laminate strength, maximum strain covering damage tolerance, flutter speed reflecting dynamic aeroelastic stability and minimum percentage of each ply orientation considering load condition uncertainties.

Under the ultimate static load, the upper boundary of FI is set as 1.0, while the maximum strain is limited to 0.004. For flutter velocity, the lower boundary is set as $1.15V_D$.

To avoid the possibility of failure of the matrix under uncertain load conditions it is desirable, but not necessarily essential, to incorporate a certain minimum number of fibres in each of the four directions. A rule-of-thumb is to make the number of laminae in each direction equal to at least 10% of the total number of laminae in the laminate part [8].

The constraint optimization problem for a minimum weight objective is expressed as follows.

$$\left\{ \begin{array}{l} \min W(X) \\ FI(X) \leq 1.0 \\ \varepsilon(X) \leq 0.004 \\ Flutter \geq 1.15V_D \\ Percentage_{0^\circ, 45^\circ, -45^\circ, 90^\circ} \geq 10\% \\ X = [t_1, t_2, \dots, t_n] \end{array} \right. \quad (8-1)$$

The detail pre-process of the optimization model will be introduced in following chapters.

8.2 Optimization Pre-process

The optimization pre-process was based on the finite element model of the outer wing box. For practical application, the whole analysis and optimization process was kept within one commercial finite element software Nastran. The optimization solution sequence (SOL200) in Nastran contains full capabilities of multidisciplinary analysis including statics, normal modes, buckling, direct and modal frequency, modal transient, static aeroelastic, and flutter analyses. [36] In this example, statics (SOL 101) and flutter (SOL 145) solution sequences were involved. In the Case Control Data of the Nastran input file (Appendix A.3), ANALYSIS = STATICS and FLUTTER commands were designated to perform corresponding type of analysis for each subcase.

8.2.1 Design Variable Definition

Because of the favourable properties of directional stiffness, composite materials offer a great potential and many advantages in the optimisation of aircraft structures. The superior properties can be achieved by optimizing the thickness of the laminate components, fibre orientations and sequences of the laminate plies.

In the initial design, the cover skins had layers in the 0° , 90° , $+45^\circ$ and -45° directions relative to material coordinate system. And they were designed symmetric and balanced forming an orthotropic nature in order to ease the design calculation and manufacturing. The laminate properties definition in Nastran input file are listed in STRUC.DAT (Appendix A.1). In the preliminary stage, optimization will only focus on laminate thickness due to its great contribution to the structure weight.

Defining the thickness of laminate components as design variables for optimization is not an easy job. For real design, one laminate consists of large number of laminae in various stacking sequence, which means each lamina

thickness (t) is a design variable. All these design variables should be changed discretely in two values $[0, t]$, because lamina thickness cannot be changed in practice unless be removed. And the whole thickness is expressed by the number of layers. This method is closest to reality, but will bring large quantity of design variables. For a large composite structure, such modelling is a heavy and fallible job for designers and more computing time is required for optimization.

In this laminate thickness optimization process, a pre-process was adopted by the author setting the laminate in blocks regardless the stacking sequence. This method gathered all laminae in the same direction together as one block. The block thickness takes place of each lamina thickness. For a symmetric layup used in this example, four blocks are formed by half laminae and the other half are kept symmetric change about the midplane. Consequently, eight blocks with only four design variables are left for each section of the skin. By doing this, the quantity of design variables were significantly reduced, therefore optimization became more efficient.

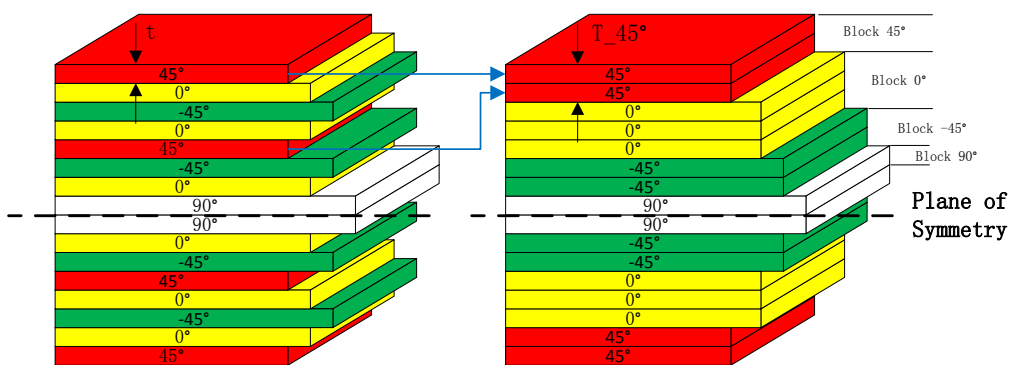


Figure 8-1 Laminate Block Definition

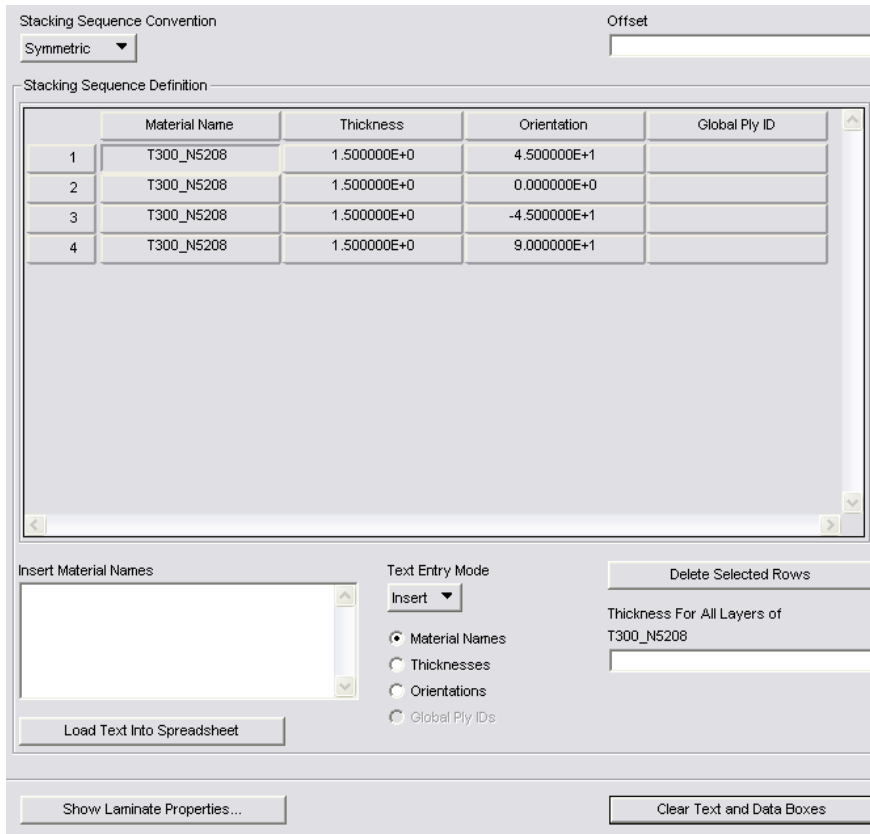


Figure 8-2 Laminate Modelling in Block

Discrete change was also adopted for each block thickness in the scale of each lamina thickness. The new design variable can be expressed as follows.

$$\left. \begin{array}{l} T_{-45^\circ} \\ T_{-0^\circ} \\ T_{-45^\circ} \\ T_{-90^\circ} \end{array} \right\} = [t, 2t, 3t, \dots, nt] \quad (8-2)$$

It is important to note that this simplified method will change the mechanical property of the laminate due to the neglect of stacking sequence. However, it is still applicable for preliminary design. This will be discussed in the last chapter.

The design model contains 72 DESVARs. Half of them control the thickness of 9 design sections for upper skin and the other half for lower skin. DDVAL entry is used to define discrete design variable values changing by the step of lamina thickness 0.125mm.

For balanced laminate characteristic, the number of plies with the angle of $+45^\circ$ and -45° should be the same. The DLINK entries are used in design variable definition to keep the thickness of $\pm 45^\circ$ equal for each design sections. Hence, the number of independent design variables for each section turned into three.

DVPREL1 entries relate the design variables to laminate block thickness.

8.2.2 Response and Constraint Definition

Design responses are used in Nastran as the basis for defining the design objective and design constraints. There are three types of responses provided in Nastran. In this example, structure weight, FI, maximum strain and flutter corresponding damping are all type-1 responses (DRESP1). They can be derived directly from each cycle analysis of the optimization process. The response type codes in DRESP1 entry are 'WEIGHT', 'CFAILURE', 'CSTRAIN' and 'FLUTTER' respectively. Percentage of each orientation for each laminate section is user-defined type-2 response (DRESP2). A simple equation is utilized to calculate it from design variable values. Structure weight response is set as the objective of optimization, while other responses are used to define design constraints.

Cautions should be paid into the element strain item code selection when defining maximum strain responses. In the subcase of statics analysis under ultimate load, the bottom skin of the wing box mainly resists tensile force. Maximum principal strain should be chosen as the response for constraint. On the other hand, the top skin reacts compressive force so that minimum principal strain with minus value should be concerned. DRESP2 entry was then used to extract the strain absolute value. In order to avoid possible numerical problem when the boundary value of strain constraint was too small, a scale factor was also introduced in the converting equation invoked by DRESP2 entry.

$$\varepsilon' = |\varepsilon| * 10^6 \quad (8-3)$$

For flutter response, flutter speed cannot be derived from analysis result directly. DRESP1 entry only selects modal damping responses at specified density, Mach number and critical velocities. A SET1 entry invoked by the DRESP1 restricted the responses to the first through the fourth modes since flutter can only happen on these first four modes. DRESP2 entries converted the damping value to a new response of the form

$$\gamma' = (\gamma - 0.03) / 0.1 \quad (8-4)$$

This form offset the response from zero and scaled it so that the constraint boundary changed to the value of -0.3. [4]

8.2.3 Optimization Constraints Definition

Design constraints are invoked by using the DCONSTR entry to impose limits on the response created before.

$$r_j^L \leq r_j(X) \leq r_j^U \quad (8-5)$$

where r_j^L is the lower bound on the j-th response and r_j^U is the corresponding upper bound.

The four original design constraints for the optimization process are shown in equation (9-1). After the converting procedure using DRESP2 entry, new constraints for the two disciplines of analyses are listed below.

Table 8-1 Design Constraints

Subcase	Constraints
ANALYSIS=STATICS	FI \leq 1.0
	$\varepsilon' \leq 4000\mu\varepsilon$
	Orientation% ≥ 0.1
ANALYSIS=FLUTTER	$\gamma' \leq -0.3$

8.3 Optimization Results

8.3.1 Optimization Process

In Nastran, a structural optimization can be described as a design loop with a number of blocks.

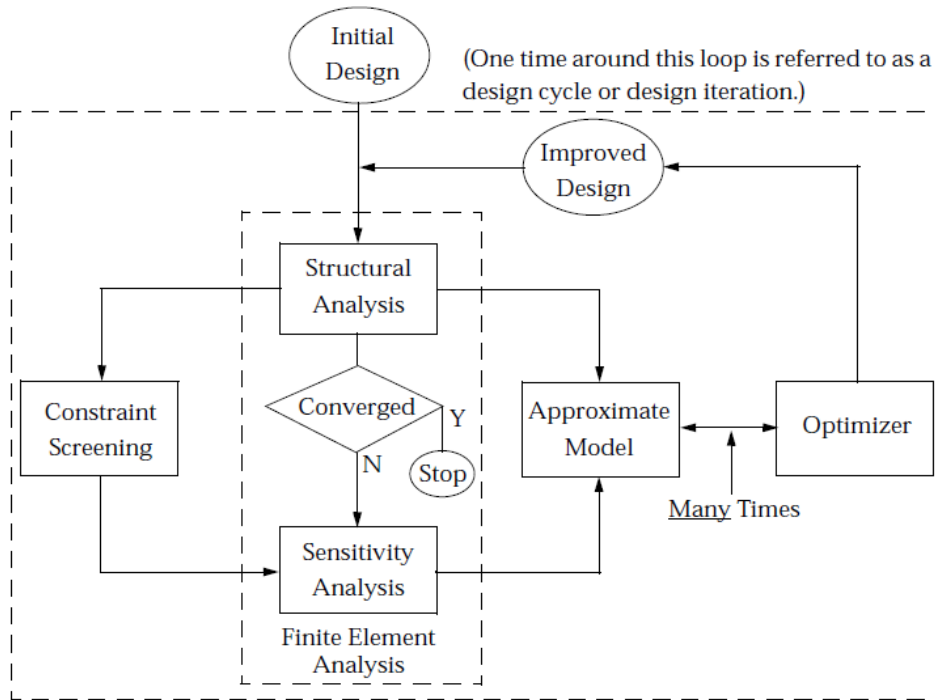
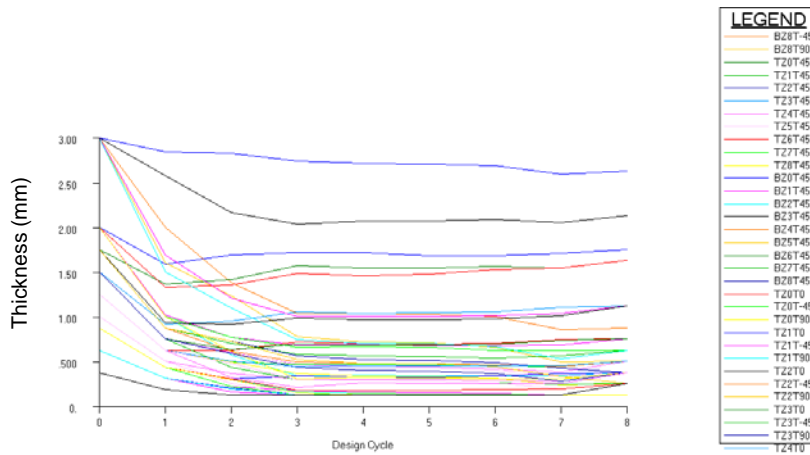
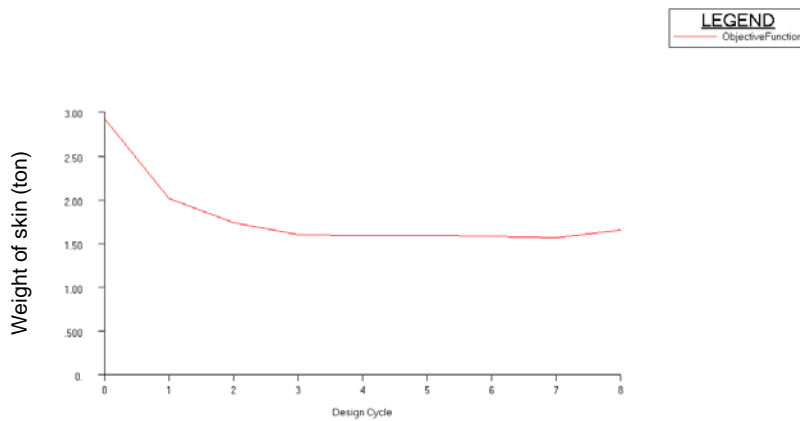


Figure 8-3 Structural Optimization Flow Chart

Turning to the results of this optimization example, the hard convergence was achieved to a feasible design since all constraints were satisfied at the optimum. The summary of design cycle history indicated that convergence was achieved in eight iterations. The design variables and objective history curves are shown in Figure 8-4.



(a) Design Variables History



(b) Optimization Objective History

Figure 8-4 Optimization History

It can be seen from the history curves that the thickness of each block for every laminate section decreased to different extent after optimization and the total skin weight had a considerable reduction.

The composite skin thickness defined by block thicknesses rather than laminae thicknesses significantly reduced the optimization computing time. The whole optimization process only cost about 3 minutes which is very efficient for a large composite wing structure. Such efficiency is absolutely meaningful in helping

designers to check the optimization model and get an ideal design modification guide quickly.

It can also be seen from the summary of design cycle history that a discrete processing analysis was completed after the eight iterations. That means, in design variable definition phase, the discrete change command for block thicknesses was performed only at the end of the optimization. Before that the block thicknesses were changing as continuous variables. This treatment can also be regarded as a trimming post-process by lamina thickness for each laminate block thickness.

8.3.2 Optimization Results Analysis

After eight design iterations, a 36% off of the skin weight was achieved which contributed a 7.7% reduction to the whole outer wing structure weight (Table 8-2).

Table 8-2 Structure Weight Comparison

Initial Structure Weight (kg)	Optimized Structure Weight (kg)	Difference
8,320	7,680	-7.7%

The optimized laminate thickness design for top and bottom skin is listed in Table 8-3. Compared with the initial size in Table 6-1, the total thickness for each design section was all decreased and the percentage for each orientation was optimized. From the comparison, a conclusion can be drawn that the initial quasi-isotropic laminate is not the optimal construction of composite wing skin for this load condition.

Table 8-3 Laminate Optimized Design

Components	Section	T(mm)	Half Block Thickness				Plies % at:		
			45	0	-45	90	0	±45	90
Top Skin	zone0	2	0.25	0.25	0.25	0.25	25.0%	50.0%	25.0%
	zone1	7.25	0.75	1.75	0.75	0.375	48.3%	41.4%	10.3%
	zone2	8.75	0.875	2.125	0.875	0.5	48.6%	40.0%	11.4%

	zone3	6.5	0.625	1.625	0.625	0.375	50.0%	38.5%	11.5%
	zone4	5.25	0.5	1.25	0.5	0.375	47.6%	38.1%	14.3%
	zone5	4.5	0.5	1	0.5	0.25	44.4%	44.4%	11.1%
	zone6	3.5	0.375	0.75	0.375	0.25	42.9%	42.9%	14.3%
	zone7	2.5	0.25	0.5	0.25	0.25	40.0%	40.0%	20.0%
	zone8	2	0.25	0.25	0.25	0.25	25.0%	50.0%	25.0%
Bottom Skin	zone0	2.25	0.375	0.25	0.375	0.125	22.2%	66.7%	11.1%
	zone1	6.5	0.625	1.625	0.625	0.375	50.0%	38.5%	11.5%
	zone2	10.5	1	2.5	1	0.75	47.6%	38.1%	14.3%
	zone3	7.5	0.75	1.75	0.75	0.5	46.7%	40.0%	13.3%
	zone4	6	0.625	1.25	0.625	0.5	41.7%	41.7%	16.7%
	zone5	4.25	0.5	0.75	0.5	0.375	35.3%	47.1%	17.6%
	zone6	3	0.375	0.5	0.375	0.25	33.3%	50.0%	16.7%
	zone7	2.25	0.25	0.375	0.25	0.25	33.3%	44.4%	22.2%
	zone8	2	0.25	0.25	0.25	0.25	25.0%	50.0%	25.0%

As the structure material was cut down after optimization, the stiffness of the wing box was reduced. Figure 8-5 gives the wing deflection diagram. The maximum displacement at wing tip was increased to 1.87 meters.

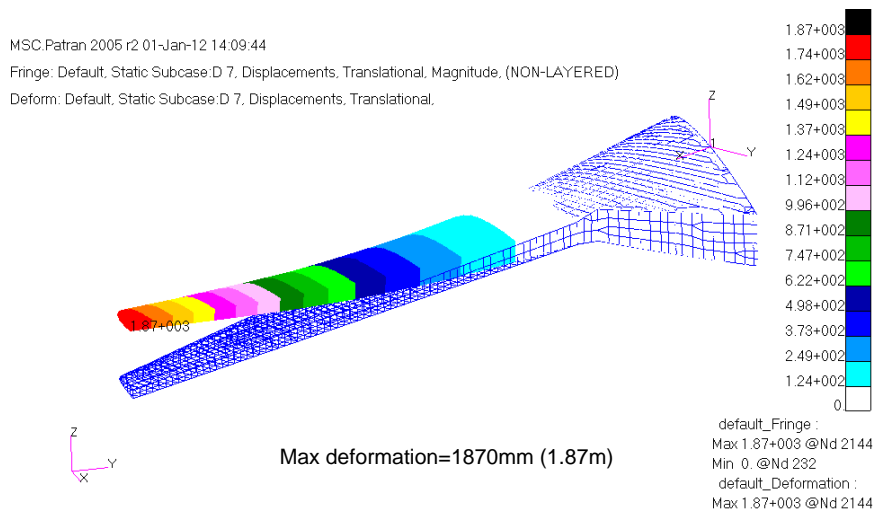


Figure 8-5 Wing Deflection after Optimization

As part of the optimization constraints, the results of maximum FI, strain level, and flutter speed can be found in Figure 8-6, Figure 8-7 and Figure 8-8. Due to

the skin thickness reduction the maximum FI was slightly increased from the initial 0.76 to 0.93, which still satisfies the strength requirement. The maximum strain was increased to 3960 $\mu\epsilon$ for both bottom and top skin which is almost equal to the constraint boundary within 1% difference. From the flutter analysis results, the optimized wing still appears bending and torsion coupling flutter. The flutter speed dropped to 585 m/s which still satisfied the aeroelastic requirement ($>1.15V_D$). Consequently, all constraints were satisfied and the allowable cut-off strain was the most crucial one in stopping the optimization cycles. In the other word, damage tolerance requirement usually provide the most strict constraint for composite wing skin design.

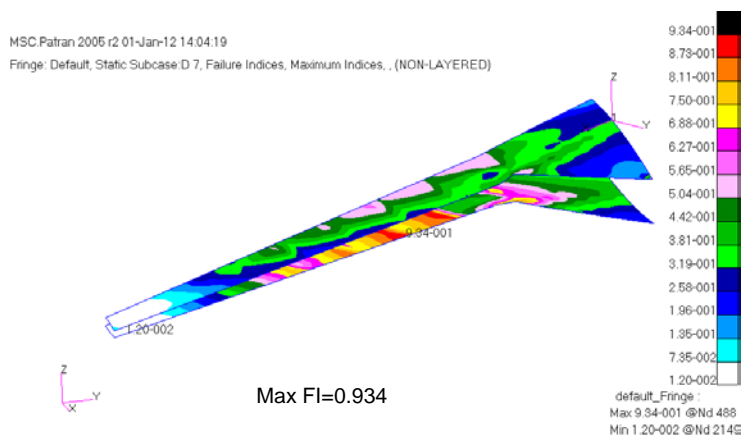
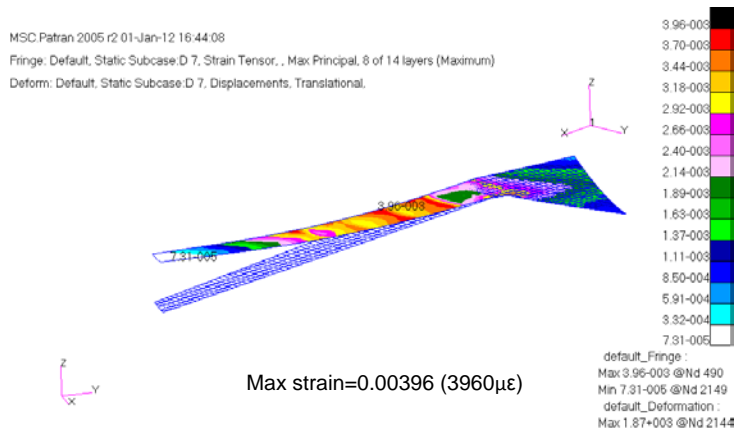
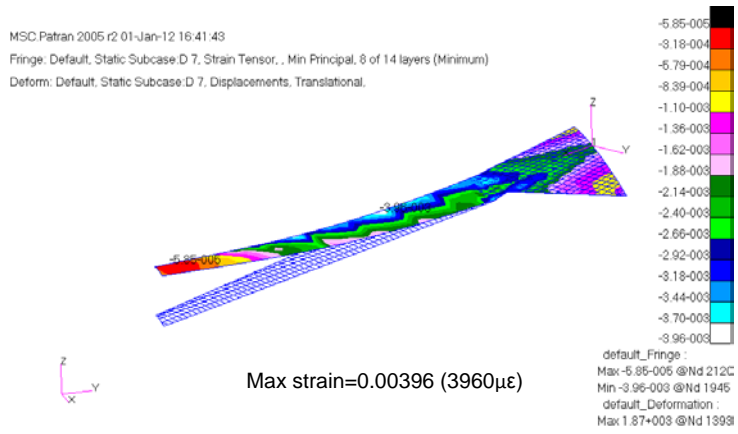


Figure 8-6 Optimized FI Result of Laminated Skin



(a) Bottom Skin



(b) Top Skin

Figure 8-7 Optimized Strain Result of Laminated Skin

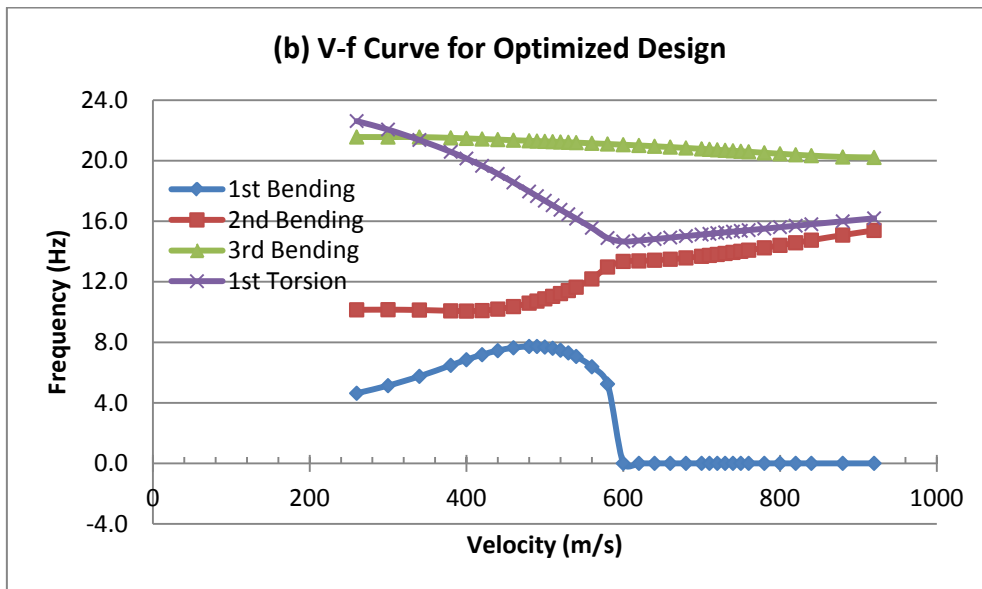
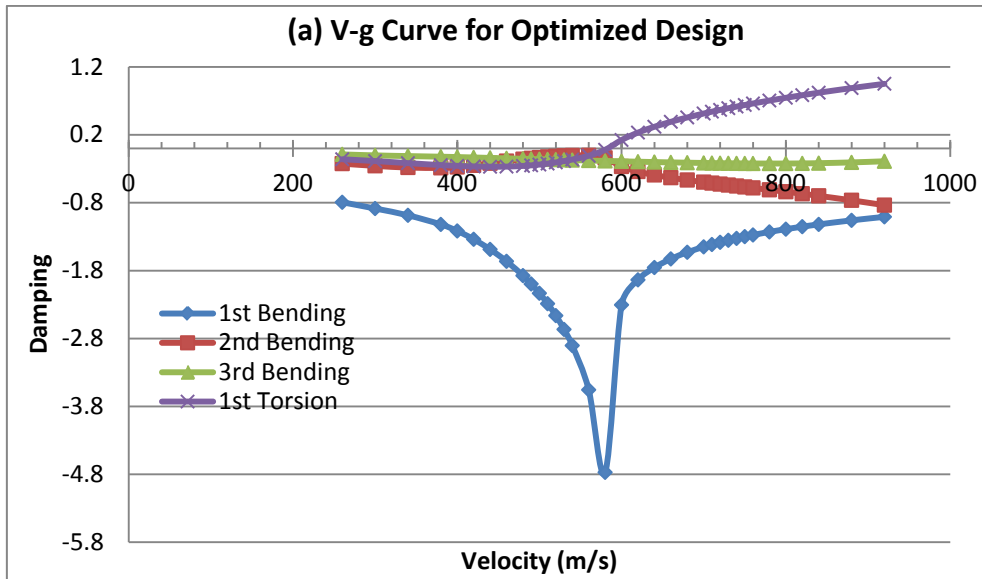


Figure 8-8 V-g and V-f Curves for Optimized Design

Figure 8-9 gives the comparison of V-g curves between the initial and final designs. It is more clearly shown that the flutter speed is declined due to the reduction of wing skin thickness by optimization approach. Because these two curves are all 1st torsion modes, the conclusion can be drawn that the critical speed is primarily dependent upon the frequency of the fundamental torsional vibration mode of the lifting surface. This is also consistent with classical bending-torsion flutter theory.

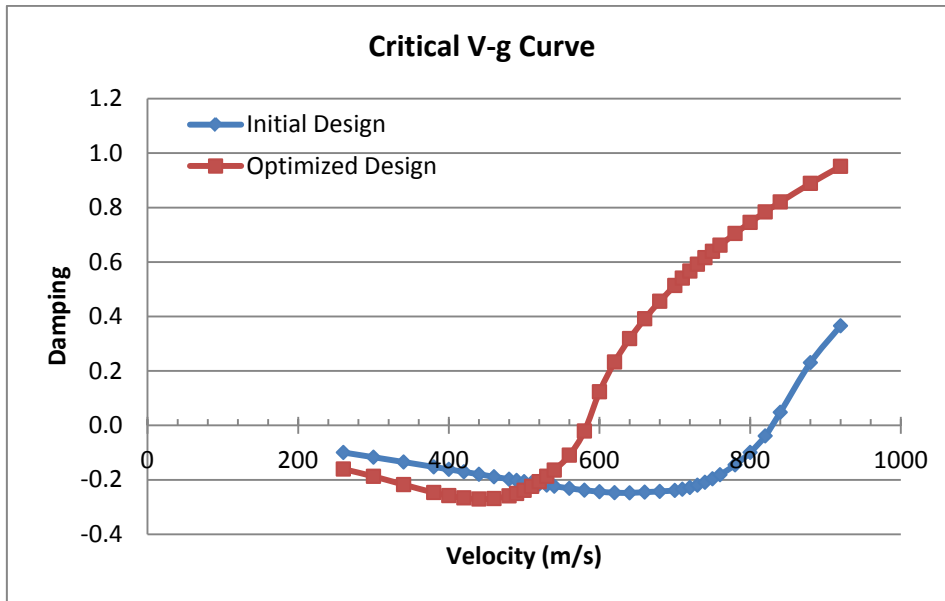


Figure 8-9 Critical V-g Curves for Optimization Comparison

8.4 Laminate Post-process

Usually, a theoretical optimal design can be obtained by the optimization process. However, when the design variables related to geometry parameter, the final values are always mathematical rather than practical. A post-process is needed to coordinate those variables to make them be of feasibility.

As mentioned before, a trimming post-process of laminate thickness has been automatically done in the optimization. This capability was achieved by defining discrete design variables related to the pre-processed laminate block thicknesses in optimization model. However, such pre-process makes the model different from the practical laminate construction because the stacking sequence is ignored. Therefore, in this research the optimization post-process will focus on the detail laminate design taking the ply sequence into account.

This work was not accomplished for all the sections of the lower and upper skin due to the time limitation. Taking the 'zone2' section of the bottom skin as the example, the laminate stacking sequence was arranged according to the optimization result. One post-process design in Table 8-4 illustrated how the

laminate blocks were broken up. In pre-process the laminate consisted of 8 symmetric blocks with total thickness of 10.5mm. While in post-process it became 84 layers of laminae with each lamina thickness of 0.125 mm. Then the new construction was defined in FE model and replaced the original laminate property.

Table 8-4 Optimization Post-process for Zone2

	Laminate Construction
Optimization Result	[45° 1mm/0° 2.5mm/-45° 1mm/90° 0.75mm] _s
Post-process	[(0/45/0/-45/0/0/45/90/-45/0/90/0/-45/0/0/45/90/-45/0/45/0) ₂] _s

After the modification, a static analysis was carried out again. By comparing the strain level diagram, the strain results for 'zone2' were almost the same. This work also proved the pre-process method used in optimization is applicable. The further discussion will be conducted in next chapter from the mechanics aspect.

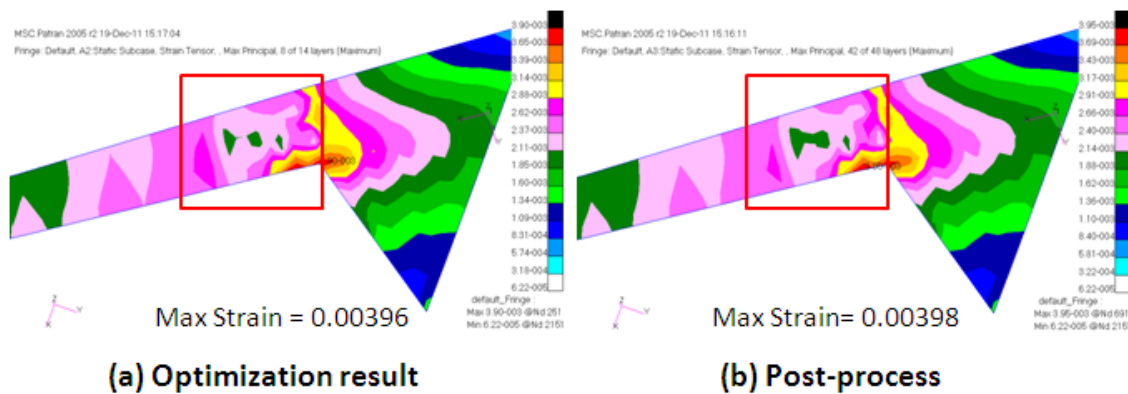


Figure 8-10 Laminate Post-process Analysis

9 Discussion and Future Work

9.1 Discussion

Discussion will continue focusing on the feasibility of the laminate thickness pre-process method. As introduced before, this method set the laminate in blocks regardless the stacking sequence. It has been proved that the optimization efficiency for a large structure can be increased since it considerably reduces the quantity of design variables. It was also proved by the FE analysis in post-process that this treatment had little influence on the laminate strain level.

In terms of classical mechanics, there are two reasons to support the FE analysis result. First reason is that all the wing skin laminates are designed and kept symmetric during optimization. This design feature allows the laminated skin have no bending-torsion coupling effect. From Figure 9-1 (ABD Matrices calculated in post-process part by NASTRAN) the 'A' matrices are exactly the same and 'B' matrices theoretically equals to zero no matter whether the skin is treated in blocks or in different laminate layup.

From the wing skin loads aspect, the global bending and torsion moment applied on the wing box are finally converted into in-plane tension or compression, and shear forces for the upper and lower skin. And the out-plane bending and torsion applied in local skin caused by the global wing deflection are much lower. Therefore, this wing skin in-plane load condition is the second reason. Under such in-plane loads, the strain level of a symmetric laminate is only determined by 'A' matrix.

Consequently, a relatively accurate result can be achieved when the skin laminate is pre-processed as blocks in this preliminary design stage. Besides, this method allows the laminate thickness change discretely in the scale of each lamina thickness and therefore makes the optimization practical.

		Membrane			Bending		
		1.15E+006	1.88E+005	0.00E+000	-6.2E-002	0.00E+000	0.00E+000
Membrane		1.88E+005	5.51E+005	-1.1E-002	0.00E+000	0.00E+000	0.00E+000
		0.00E+000	-1.1E-002	2.33E+005	0.00E+000	0.00E+000	0.00E+000
		-6.2E-002	0.00E+000	0.00E+000	1.14E+007	2.19E+006	1.80E+006
Bending		0.00E+000	0.00E+000	0.00E+000	2.19E+006	3.30E+006	1.80E+006
		0.00E+000	0.00E+000	0.00E+000	1.80E+006	1.80E+006	2.61E+006

(a) ABD Matrix for Pre-process

		Membrane			Bending		
		1.15E+006	1.88E+005	0.00E+000	0.00E+000	-7.0E-003	0.00E+000
Membrane		1.88E+005	5.51E+005	-1.1E-002	-7.0E-003	-5.4E-002	0.00E+000
		0.00E+000	-1.1E-002	2.33E+005	0.00E+000	0.00E+000	1.17E-002
		0.00E+000	-7.0E-003	0.00E+000	1.13E+007	1.72E+006	1.02E+005
Bending		-7.0E-003	-5.4E-002	0.00E+000	1.72E+006	4.37E+006	1.02E+005
		0.00E+000	0.00E+000	1.17E-002	1.02E+005	1.02E+005	2.13E+006

(b) ABD Matrix for Post-process

Figure 9-1 ABD Matrices Comparison

9.2 Future Work

This thesis takes a flying wing airliner as an example in order to present a preliminary design and optimization technique for large composite wing structures. Actually, from the point of structural integrity in practical engineering, a feasible design should meet all kinds of requirements. In this optimization process, multiple constraints only include composite strength, damage tolerance and flutter because of time limitation. In the future work, more considerations can be added to enrich the process and make the technique more practical. Taking the buckling requirements as an example, it is always an important constraint especially for the top skin panels which generally resist compression forces. As a multidisciplinary optimization tool, NASTRAN can effectively help designers manage to accomplish it.

In the FE model of this example, the properties of composite internal substructures were defined with equivalent isotropic elastic constant. In future work, laminate properties can be modelled to carry out more detailed analysis.

For optimization, the internal substructure was also designed conservative, and can be optimized to achieve extra weight reduction.

Due to the anisotropic nature, composite materials provide more potential in structure optimization. In this preliminary design stage, laminate thickness was optimized to achieve weight saving. However, more benefits can be obtained by tailoring the laminates. At following detail design stage, ply orientation and stacking sequence can be set as design variables. Since this would not change the structure weight, the stiffness or flutter features can be set as the new objectives so that better performance can be got without paying weight penalty.

10 Conclusion

In this thesis, efforts have been made to optimize a large composite wing structure for minimum weight subject to multiple design constraints. It has been demonstrated that based on the initial sizing, the whole structure FE analysis and optimization process can be implemented by employing the commercial package Nastran. An optimized wing structure with detailed FE model can be obtained automatically and efficiently by this approach. In addition, the following conclusions can be drawn.

1. The structure initial sizing by Denis Howe's method is to some extent conservative and overestimated. And for a structure designed through routine process, a significant structure weight reduction can still be achieved by the optimization technique subject to multiple design constraints;
2. For practical application, the methodology and technique keep the whole FE modelling, analysis and optimization process within one commercial package by making full use of NASTRAN code.
3. The pre-process method setting laminate thickness in block is proved to be efficient with little compromise of accuracy for the optimization of a large composite wing structure in preliminary design stage;
4. Using discrete design variable for laminate thickness optimization can reduce the work demand for trimming the ply number and thickness in post-process and therefore make the optimization more efficient and practical;
5. In the application of composite material to structures, the allowable strain level considering damage tolerance plays an important role on the composite structure design. In a multi-constraint optimization process, the maximum strain requirement is usually more critical than the stress and aeroelastic criteria and hence drives the structure design.

REFERENCES

1. Crane D, "Dictionary of Aeronautical Terms (third edition)", Aviation Supplies & Academics, 1997.
2. Matthews F L, Davies G A O, Hitchings D and Soutis C, "Finite element modelling of composite materials and structures", Woodhead Publishing Limited, 2000.
3. Oyibo G A, "A unified flutter analysis for composite aircraft wings", 25TH AIAA/ASME/ASCE/AHS Structures, Structural Dynamics and Materials Conference. New York: AIAA, 1984.
4. "Aeroelastic analysis user's guide", MSC. Nastran Version 68, MSC. Software Corporation.
5. Cole S R, Nagaraja K S and Rivera J A, "Flutter study of an advanced composite wing with external stores" 28th AIAA/ASME/ASCE/AHS Structures, Structural Dynamics and Materials Conference and AIAA Dynamics Specialists Conference. Part 2. - New York: AIAA, 1987.
6. Chowdary T V R, Parthan S and Sinha P K, "Finite element flutter analysis of laminated composite panels", Computers & Structures, 1994.
7. Qin Z, Marzocca P, Librescu L, Aeroelastic instability and response of advanced aircraft wings at subsonic flight speeds, Aerospace Sci Technol; 6:195-208, 2002.
8. Niu M, "Composite Airframe Structures: practical design information and data", Hong Kong Conmilit Press Ltd, 1999.
9. Schmit, L.A and Farshi, B. "Optimum design of laminated fibre composite plates". International journal for numerical methods in engineering, 1977.
10. Almeida F S and Awruch A M, "Design optimization of composite laminated structures using genetic algorithms and finite element analysis", Composite Structures, vol. 88, no. 3, pp. 443-454, 2009.
11. Walker M and Smith RE, "A technique for the multi-objective optimisation of laminated composite structures using genetic algorithms and finite element analysis", Composite Structures 62, 123–128, 2003.

12. Honda S, Narita Y, Sasaki K, "Discrete Optimization for Vibration Design of Composite Plates by Using Lamination Parameters", *Advanced Composite Materials* 18, 297–314, 2009.
13. Kere P, Lyly M and Koski J, "Using multicriterion optimization for strength design of composite laminates", *Composite Structures*, vol. 62, no. 3-4, pp. 329-333, 2003.
14. Zehnder N and Ermanni P, "A methodology for the global optimization of laminated composite structures", *Composite Structures*, vol. 72, no. 3, pp. 311-320, 2006.
15. Narayana N G, Gopalakrishnan S, Ganguli R, "Design optimization of composites using genetic algorithms and failure mechanism based failure criterion", *Compos Struct*; 83(4): 354-367. 2008.
16. Lopez, R. H., Luersen, M. A. and Cursi, E. S. (2009), "Optimization of laminated composites considering different failure criteria", *Composites Part B: Engineering*, vol. 40, no. 8, pp. 731-740.
17. Wang L, Williams AF, Llamas R, "Aircraft wing structural optimisation with manufacturing considerations", AIAA-2000-4842.
18. Liu D, Toropov V V, Querin O M and Barton D C, "Bi-level Optimization of Blended Composite Panels", *AIAA Journal*, AIAA 2009-2182, May 2009.
19. Guo S, Banerjee J R, Cheung C W, "The effect of laminate lay-up on the flutter speed of composite wings", *Proc. IMechE, Part G: J Aerospace Eng* 2003; 217: 115-122.
20. Guo S, Cheng W and Cui D, "Optimization of Composite Wing Structures for Maximum Flutter Speed", 46th AIAA/ASME/ASCE/AHS/ASC Structures, Structural Dynamics & Materials Conference 18 - 21 April 2005.
21. Guo S, Chen W and Cui D, "Aeroelastic tailoring of composite wing structures by laminate layup optimization", *AIAA J* 2006; 44: 3146-149.
22. Lillico M, Butler R, Guo S, Banerjee JR. "Aeroelastic optimization of composite wings using the dynamic stiffness method", *Aeronaut J* 1997; 101: 77-86.

23. Guo S, Li D and Liu Y, "Multi Objective Optimization of a Composite Wing Subject to Strength and Aeroelastic Constraints", Proc. IMechE Vol. 0 Part G: J. Aerospace Engineering, Oct 21, 2011.
24. Guo S. "Aeroelastic optimization of an aerobatic aircraft wing structure", *Aerosp Sci Technol* 2007; 11: 396-404.
25. "Failure criteria and laminate strength prediction" (2003), available at: <http://www.admc.esrtechnology.com/Background/Failure/>.
26. Niu M, "Airframe structural design: practical design information and data on aircraft structures", Hong Kong Conmilit Press Ltd. 1999.
27. Howe D, "Aircraft loading and structural layout", American Institute of Aeronautics and Astronautics, Inc, 2004.
28. Hart Smith, "The ten-percent rule", *Aerospace Materials*, 5(2), August/October 1993.
29. Tsai S W, Wu E M, "A general theory of strength for anisotropic materials", *J. Compos. Mater.*, 1971, 5, 58–80.
30. Albano E and Rodden W P, "A Doublet Lattice Method for Calculating Lift Distributions on Oscillating Surfaces in Subsonic Flows". *AIAAJ.*, Vol. 7 pp279-285 p. 2192 1969
31. Mukhopadhyay V, "Blended-Wing-Body (BWB) Fuselage Structural Design for Weight Reduction", AIAA, 2005.
32. Tetlow R, "Design Charts for Carbon-fibre Composites", Cranfield Memo No. 9. 1970.
33. Guo S, "USER MANUAL FOR PROGRAM ABDMXS.EXE".
34. Niu M, "Airframe Stress Analysis and Sizing (2nd edition)", Hong Kong Conmilit Press Ltd, 1999.
35. European Aviation Safety Agency, "Certification Specifications for Large Aeroplanes CS-25", Amendment 3, 19 September 2007
36. "Design Sensitivity and Optimization User's Guide", MSC. Nastran Version 68, MSC. Software Corporation.
37. "Flying Wing Airliner FW-11 Group Project Specification", Cranfield University, 2011

APPENDICES

Appendix A Optimization Model Input File

The Nastran Bulk Data entries of the optimization model are listed in this appendix. The whole model is divided into several input files. The main optimization control codes are contained in 'FW11_COMP_WING_OPTIM.bdf' in A.4. Structure and mass data are shown in 'FW11_STRUCT_COMP.DAT' in A.1. The loads data for static analysis are illustrated 'FW11_LOADS.DAT' in A.2. And the flutter control code and aerodynamic model are listed in 'FW11_FLUTTER.DAT' in A.3. All the input files listed here are just some fragments.

A.1 Structure Codes

Table A-1 FW11_STRUCT_COMP.DAT

```
$ Structure Data of FW11 Outer Wing with Composite Skin
$
$ Referenced Coordinate Frames For Composite Skins
CORD2R 1          15823.1 -12400. 1205.58 15823.1 -12400. 21344.7
          26854.9 -29248.9 1205.58
$
$ Material Record : T300_N5208
MAT8 2  181000. 10300. .28  7170. 7170. 5000. 1.6-9
          1500. 1500. 40.  246. 68.
$
$ Elements and Element Properties for region : TOP_SKIN_ZONE0
$ Composite Material Description :
PCOMP 29          50.  TSAI 0.  0.  SYM
      2  1.  45.  YES  2  1.  0.  YES
      2  1. -45.  YES  2  1.  90. YES
$ Elements and Element Properties for region : TOP_SKIN_ZONE1
$ record : UPPER_1
$ Composite Material Description :
PCOMP 28          50.  TSAI 0.  0.  SYM
      2  1.5 45.  YES  2  1.5 0.  YES
      2  1.5 -45. YES  2  1.5 90. YES
$ Elements and Element Properties for region : TOP_SKIN_ZONE2
$ record : UPPER_2
$ Composite Material Description :
PCOMP 3           50.  TSAI 0.  0.  SYM
      2  2.0 45.  YES  2  2.0 0.  YES
      2  2.0 -45. YES  2  2.0 90. YES
...
$
$ Elements and Element Properties for region : BOTTOM_SKIN_ZONE0
$ record : LOWER_0
```

```

$ Composite Material Description :
PCOMP 36          50.  TSAI 0.  0.  SYM
      2  1.  45.  YES  2  1.  0.  YES
      2  1. -45.  YES  2  1.  90. YES
$ Elements and Element Properties for region : BOTTOM_SKIN_ZONE1
$ record : LOWER_1
$ Composite Material Description :
PCOMP 16          50.  TSAI 0.  0.  SYM
      2  1.5 45.  YES  2  1.5 0.  YES
      2  1.5 -45. YES  2  1.5 90. YES
$ Elements and Element Properties for region : BOTTOM_SKIN_ZONE2
$ record : LOWER_2
$ Composite Material Description :
PCOMP 6           50.  TSAI 0.  0.  SYM
      2  2.0 45.  YES  2  2.0 0.  YES
      2  2.0 -45. YES  2  2.0 90. YES
...
$
$
$ Elements and Element Properties for region : STRINGER
PBARL 2  1  1
      60. 60. 50. 2. 4. 3.
$ Pset: "STRINGER" will be imported as: "pbarl.2"
CBAR 3985 2 1668 1491 0. 0. 1.
CBAR 3986 2 1491 1856 0. 0. 1.
CBAR 3987 2 1856 1857 0. 0. 1.
CBAR 3988 2 1857 1498 0. 0. 1.
CBAR 3989 2 1498 1870 0. 0. 1.
...
$
$ Pset: "TOP_SKIN_ZONE2" will be imported as: "pcomp.3"
CQUAD4 264 3 1484 1485 1853 1851 1
CQUAD4 265 3 1853 1852 1850 1851 1
CQUAD4 266 3 1852 1496 1495 1850 1
CQUAD4 267 3 1485 1486 1855 1853 1
CQUAD4 268 3 1855 1854 1852 1853 1
CQUAD4 269 3 1854 1497 1496 1852 1
...
$ Nodes of the Entire Model
GRID 1 13736.3 -13046.6-852.731
GRID 2 13987.2 -12882.3-900.413
GRID 3 14238.2 -12717.9-944.646
GRID 4 14489.2 -12553.5-985.974
GRID 5 13506.9 -13196.9-805.51
GRID 6 14256.8 -13841.3-740.06
...
$
$
$ Mass of Control Surfaces
$
$ Elements and Element Properties for region : mass_split_drag_rudder
CONM2 102081 1629 .0072
CONM2 102082 230 .0072
CONM2 102083 1624 .0072
CONM2 102084 225 .0072
CONM2 102085 1619 .0072
CONM2 102086 220 .0072
CONM2 102087 1614 .0072

```

CONM2	102088	215	.0072
CONM2	102089	1609	.0072
CONM2	102090	211	.0072
CONM2	102091	1604	.0072
CONM2	102092	206	.0072
CONM2	102093	1598	.0072
CONM2	102094	200	.0072
\$ Elements and Element Properties for region : mass_aileron			
CONM2	102095	1592	.0116
CONM2	102096	194	.0116
CONM2	102097	1586	.0116
CONM2	102098	188	.0116
CONM2	102099	1580	.0116
CONM2	102100	182	.0116
CONM2	102101	1574	.0116
CONM2	102102	176	.0116
CONM2	102103	1568	.0116
CONM2	102104	171	.0116
CONM2	102105	1562	.0116
CONM2	102106	165	.0116
\$ Elements and Element Properties for region : mass_flap			
CONM2	102107	1555	.016
CONM2	102108	158	.016
CONM2	102109	1548	.016
CONM2	102110	151	.016
CONM2	102111	1541	.016
CONM2	102112	144	.016
CONM2	102113	1534	.016
CONM2	102114	137	.016
CONM2	102115	1527	.016
CONM2	102116	131	.016
CONM2	102117	1520	.016
CONM2	102118	124	.016
CONM2	102119	1512	.016
CONM2	102120	116	.016
CONM2	102121	1504	.016
CONM2	102122	108	.016
CONM2	102123	1665	.016
CONM2	102124	252	.016
\$ Elements and Element Properties for region : mass_outer_elevator			
CONM2	102125	1664	.038
CONM2	102126	251	.038
CONM2	102127	1483	.038
CONM2	102128	2510	.038
CONM2	102129	87	.038
CONM2	102130	1468	.038
CONM2	102131	2513	.038
CONM2	102132	2515	.038
CONM2	102133	71	.038

A.2 Static Loads Codes

Table A-2 FW11_LOADS.DAT

```

$ Loads for Static Analysis
SPCADD 2 1 3
LOAD 3 3.75 1. 2 1. 4 1. 5
1. 6 1. 7 1. 8 1. 9
1. 10 1. 11 1. 12 1. 13
1. 14 1. 15 1. 16 1. 17
1. 18 1. 19 1. 20 1. 21
1. 22 1. 23 1. 24 1. 25
1. 26 1. 27 1. 28 1. 29
1. 30 1. 31 1. 32 1. 33
1. 34 1. 35 1. 36 1. 37
$ Displacement Constraints of Load Set : spc1.1
SPC1 1 123456 232 THRU 240
SPC1 1 123456 243 245 247 249 662
SPC1 1 123456 804 THRU 814
SPC1 1 123456 816 971 972 973 974 975
976 979 1306 1310 1392 1405 1429 1631
1632 1633 1634 1635 1637 1639 1642 1644
1646 1648 1650 1652 1653 1655 1657 1660
1662 1666 2136 2137 2179 2180 2181 2188
2190 2191 2193 2196 2199 2200 2201 2242
2243 2244 2245 2246 2247 2321 2324 2325
2326 2327 2328 2329 2483 2484 2485 2486
2487 2544 2545 2550 2551
SPC1 1 123456 2554 THRU 2736
$ Displacement Constraints of Load Set : spc2
SPC1 3 1 1393 1541 1592
$ Nodal Forces of Load Set : f2
FORCE 11 1628 0 4646.8 0. 0. 1.
$ Nodal Forces of Load Set : f3~5
FORCE 22 1615 0 4428.8 0. 0. 1.
FORCE 22 1618 0 4428.8 0. 0. 1.
FORCE 22 1623 0 4428.8 0. 0. 1.
$ Nodal Forces of Load Set : f6
FORCE 23 1610 0 7193.5 0. 0. 1.
$ Nodal Forces of Load Set : f7~8
FORCE 24 1599 0 8826.8 0. 0. 1.
FORCE 24 1603 0 8826.8 0. 0. 1.
$ Nodal Forces of Load Set : f9
FORCE 25 1593 0 9723.9 0. 0. 1.
$ Nodal Forces of Load Set : f10
FORCE 2 1587 0 10589.9 0. 0. 1.
$ Nodal Forces of Load Set : f11
FORCE 4 1581 0 11049. 0. 0. 1.
$ Nodal Forces of Load Set : f12~13
FORCE 5 1569 0 11932.4 0. 0. 1.
FORCE 5 1575 0 11932.4 0. 0. 1.
$ Nodal Forces of Load Set : f14
FORCE 6 1563 0 12372. 0. 0. 1.
$ Nodal Forces of Load Set : f15~16
FORCE 7 1549 0 13056. 0. 0. 1.
FORCE 7 1556 0 13056. 0. 0. 1.
$ Nodal Forces of Load Set : f17

```

FORCE 8	1542	0	13818.1	0.	0.	1.
\$ Nodal Forces of Load Set : f18						
FORCE 9	1535	0	14119.5	0.	0.	1.
\$ Nodal Forces of Load Set : f19						
FORCE 10	1041	0	14162.	0.	0.	1.
\$ Nodal Forces of Load Set : f20~21						
FORCE 12	747	0	15132.1	0.	0.	1.
FORCE 12	750	0	15132.1	0.	0.	1.
\$ Nodal Forces of Load Set : f22						
FORCE 13	741	0	15486.1	0.	0.	1.
\$ Nodal Forces of Load Set : f23						
FORCE 14	735	0	16095.8	0.	0.	1.
\$ Nodal Forces of Load Set : f24						
FORCE 15	728	0	16859.9	0.	0.	1.
\$ Nodal Forces of Load Set : f25						
FORCE 16	1020	0	18382.8	0.	0.	1.
\$ Nodal Forces of Load Set : f26						
FORCE 17	1467	0	21147.	0.	0.	1.
\$ Nodal Forces of Load Set : f27						
FORCE 18	1430	0	21465.	0.	0.	1.
\$ Nodal Forces of Load Set : f28						
FORCE 19	1415	0	21759.4	0.	0.	1.
\$ Nodal Forces of Load Set : f29						
FORCE 20	1407	0	22068.5	0.	0.	1.
\$ Nodal Forces of Load Set : f30						
FORCE 21	1396	0	25799.3	0.	0.	1.
\$ Nodal Forces of Load Set : w1						
FORCE 26	1638	0	1045.5	0.	0.	-1.
\$ Nodal Forces of Load Set : w2~5						
FORCE 35	1613	0	32.5	0.	0.	-1.
FORCE 35	1617	0	32.5	0.	0.	-1.
FORCE 35	1622	0	32.5	0.	0.	-1.
FORCE 35	1627	0	32.5	0.	0.	-1.
\$ Nodal Forces of Load Set : w6~8						
FORCE 36	1596	0	70.4	0.	0.	-1.
FORCE 36	1602	0	70.4	0.	0.	-1.
FORCE 36	1608	0	70.4	0.	0.	-1.
\$ Nodal Forces of Load Set : w9~10						
FORCE 37	1585	0	90.	0.	0.	-1.
FORCE 37	1590	0	90.	0.	0.	-1.
\$ Nodal Forces of Load Set : w11						
FORCE 27	1579	0	811.1	0.	0.	-1.
\$ Nodal Forces of Load Set : w12~13						
FORCE 28	1567	0	1351.	0.	0.	-1.
FORCE 28	1573	0	1351.	0.	0.	-1.
\$ Nodal Forces of Load Set : w14~16						
FORCE 29	1547	0	1686.4	0.	0.	-1.
FORCE 29	1553	0	1686.4	0.	0.	-1.
FORCE 29	1560	0	1686.4	0.	0.	-1.
\$ Nodal Forces of Load Set : w17~19						
FORCE 30	1526	0	2059.	0.	0.	-1.
FORCE 30	1533	0	2059.	0.	0.	-1.
FORCE 30	1540	0	2059.	0.	0.	-1.
\$ Nodal Forces of Load Set : w20~21						
FORCE 31	1510	0	2469.	0.	0.	-1.
FORCE 31	1518	0	2469.	0.	0.	-1.
\$ Nodal Forces of Load Set : w22~24						
FORCE 32	1470	0	2916.2	0.	0.	-1.

FORCE	32	1485	0	2916.2	0.	0.	-1.
FORCE	32	1496	0	2916.2	0.	0.	-1.
FORCE	32	1503	0	2916.2	0.	0.	-1.
\$ Nodal Forces of Load Set : w25							
FORCE	33	1450	0	3595.7	0.	0.	-1.
\$ Nodal Forces of Load Set : w26~28							
FORCE	34	1412	0	4563.	0.	0.	-1.
FORCE	34	1420	0	4563.	0.	0.	-1.
FORCE	34	1434	0	4563.	0.	0.	-1.

A.3 Flutter Modelling Codes

Table A-3 FW11_FLUTTER.DAT

```

$ Flutter Analysis Input of FW11 Outer Wing with Composite Skin
$
$ Global Data for Steady Aerodynamics
$
$ A half-span model is defined
AERO 0 1. 11750. 1.225-12
$
$ Flat Aero Surface: inner_lifting_surface
PAERO1 103001
CAERO1 103001 103001 0 4 7 1
7300.165-8700. -7.85-1320000. -.000404.0003565-7.85-1327300.
$
$ Flat Aero Surface: middle_lifting_surface
PAERO1 102001
CAERO1 102001 102001 0 6 7 1
14432.51-17200. -1.69-136344. 7300.165-8700. -7.85-1320000.
$
$ Flat Aero Surface: outer_lifting_surface
PAERO1 101001
CAERO1 101001 101001 0 20 7 1
27690.29-33000. -1.69-132500. 14432.51-17200. -1.69-136344.
$
$ Surface Spline:
AELIST 1 102001 102002 102003 102004 102005 102006 102007
102008 102009 102010 102011 102012 102013 102014 102015
102016 102017 102018 102019 102020 102021 102022 102023
102024 102025 102026 102027 102028
SET1 1 692 693 694 695 696 697 704
705 706 707 708 709 804 805 806
807 808 809 983 984 985 986 987
992 993 994 995 1001 1002 1075 1328
1392 1395 1396 1397 1398 1399 1400 1401
1402 1403 1404 1405 1406 1407 1408 1409
1410 1411 1412 1413 1414 1415 1416 1417
1418 1419 1420 1421 1422 1423 1424 1425
1426 1427 1428 1429 1430 1431 1432 1433
1434 1435 1436 1437 1438 1439 1440 1441
1442 1443 1444 1445 1446 1447 1449 1450
1451 1452 1453 1454 1455 1456 1457 1458
1459 1460 1461 1462 1463 1464 1465 1466
1468 1475 1476 1477 1478 1479 1480 1481

```



```

1631 1632 1633 1634 1635 1637 1639 1642
1644 1645 1646 1647 1648 1649 1650 1651
1652 1653 1654 1655 1656 1657 1658 1659
1660 1661 1662 1663 2321 2551
SPLINE4 11 102001 1 1 0. IPS BOTH
$
$ Surface Spline:
AELIST 2 101001 101002 101003 101004 101005 101006 101007
101008 101009 101010 101011 101012 101013 101014 101015
101016 101017 101018 101019 101020 101021 101022 101023
101024 101025 101026 101027 101028 101029 101030 101031
101032 101033 101034 101035 101036 101037 101038 101039
101040 101041 101042 101043 101044 101045 101046 101047
101048 101049 101050 101051 101052 101053 101054 101055
101056 101057 101058 101059 101060 101061 101062 101063
101064 101065 101066 101067 101068 101069 101070 101071
101072 101073 101074 101075 101076 101077 101078 101079
101080 101081 101082 101083 101084 101085 101086 101087
101088 101089 101090 101091 101092 101093 101094 101095
101096 101097 101098 101099 101100 101101 101102 101103
101104 101105 101106 101107 101108 101109 101110 101111
101112 101113 101114 101115 101116 101117 101118 101119
101120 101121 101122 101123 101124 101125 101126 101127
101128 101129 101130 101131 101132 101133 101134 101135
101136 101137 101138 101139 101140
SET1 2 719 725 726 728 729 730 735
736 741 742 747 748 749 750 751
752 753 754 755 756 757 758 759
762 763 764 768 769 773 776 779
780 784 785 789 795 798 801 999
1000 1006 1007 1008 1009 1010 1015 1020
1021 1023 1024 1026 1027 1029 1035 1041
1042 1043 1051 1053 1061 1063 1065 1067
1068 1069 1072 1073 1074 1393 1394 1448
1467 1469 1470 1471 1472 1473 1474 1482
1484 1485 1486 1487 1488 1489 1490 1491
1492 1493 1494 1495 1496 1497 1498 1499
1500 1501 1502 1503 1504 1505 1506 1507
1508 1509 1510 1511 1512 1513 1514 1515
1516 1517 1518 1519 1520 1521 1522 1523
1524 1525 1526 1527 1528 1529 1530 1531
1532 1533 1534 1535 1536 1537 1538 1539
1540 1541 1542 1543 1544 1545 1546 1547
1548 1549 1550 1551 1552 1553 1554 1555
1556 1557 1558 1559 1560 1561 1562 1563
1564 1565 1566 1567 1568 1569 1570 1571
1572 1573 1574 1575 1576 1577 1578 1579
1580 1581 1582 1583 1584 1585 1586 1587
1588 1589 1590 1591 1592 1593 1594 1595
1596 1597 1598 1599 1600 1601 1602 1603
1604 1605 1606 1607 1608 1609 1610 1611
1612 1613 1614 1615 1616 1617 1618 1619
1620 1621 1622 1623 1624 1625 1626 1627
1628 1629 1630 1636 1638 1640 1641 1643
1664 1665
SPLINE4 10 101001 2 2 0. IPS BOTH
$
$-----

```

```

$ Flutter Control
$-----
$
EIGRL,10,,,5
PARAM,LMODES,5
PARAM,VREF,1000.
$
MKAERO1,0.0
,0.01,0.1,0.3,0.5,0.7,0.8,0.9,1.0
MKAERO1,0.0
,1.2,1.5,2.0,3.0,4.0,6.0,8.0,10.0
$
FLUTTER,9,PK,1,2,3,,5
$
FLFACT,1,1.0
FLFACT,2,0.0
FLFACT,3,260000.,300000.,340000.,380000.,400000.,420000.,440000.
,460000.,480000.,490000.,500000.,510000.,520000.,530000.,540000.
,560000.,580000.,600000.,620000.,640000.,660000.,680000.,700000.
,710000.,720000.,730000.,740000.,750000.,760000.,780000.,800000.
,820000.,840000.,880000.,920000.
$

```

A.4 Optimization Modelling Codes

Table A-4 FW11_COMP_WING_OPTIM.bdf

```

$ Optimization for Composite Wing under Multi-constraint, Database
$ TIME 10
SOL 200
CEND
$
TITLE = Optimization under Multi-constraint
SUBTITLE = FW-11 Outer Wing Struct
ECHO = NONE
SPC = 2
DESOBJ(MIN) = 30000
SUBCASE 1
  SUBTITLE=Static Analysis
  ANALYSIS=STATICS
  LOAD = 3
  DISPLACEMENT=ALL
  STRESS=ALL
  STRAIN=ALL
  FORCE=ALL
  DESSUB = 40001
SUBCASE 2
  ANALYSIS=FLUTTER
  LABEL = Flutter Analysis
  METHOD = 10
  FMETHOD = 9
  DESSUB = 40002
BEGIN BULK
$

```

```

PARAM,POST,-1
PARAM,GRDPNT,0
PARAM,PRTMAXIM,YES
PARAM,NOCOMPS,0
$
$ Structure Data
INCLUDE FW11_STRUCT_COMP.DAT
$ Mass Data
INCLUDE FW11_MASS_1116.DAT
$ External Loads Data
INCLUDE FW11_LOADS_1202.DAT
$
$-----
$ DESIGN MODEL:
$-----
$
$...Define Design Variables
$ Top Skin Thickness for Zones
DESVAR,10001,TZ0T45,1.0,0.125,10.0,,1
DESVAR,10002,TZ0T0,1.0,0.125,10.0,,1
DESVAR,10003,TZ0T-45,1.0,0.125,10.0,,1
DESVAR,10004,TZ0T90,1.0,0.125,10.0,,1
DESVAR,10005,TZ1T45,1.5,0.125,10.0,,1
DESVAR,10006,TZ1T0,1.5,0.125,10.0,,1
DESVAR,10007,TZ1T-45,1.5,0.125,10.0,,1
DESVAR,10008,TZ1T90,1.5,0.125,10.0,,1
...
$ Bottom Skin Thickness for Zones
DESVAR,10101,BZ0T45,1.0,0.125,10.0,,1
DESVAR,10102,BZ0T0,1.0,0.125,10.0,,1
DESVAR,10103,BZ0T-45,1.0,0.125,10.0,,1
DESVAR,10104,BZ0T90,1.0,0.125,10.0,,1
DESVAR,10105,BZ1T45,1.5,0.125,10.0,,1
DESVAR,10106,BZ1T0,1.5,0.125,10.0,,1
DESVAR,10107,BZ1T-45,1.5,0.125,10.0,,1
DESVAR,10108,BZ1T90,1.5,0.125,10.0,,1
...
$
$...Define Discrete Changes of Ply Thickness
DDVAL,1,0.125,THRU,10.0,BY,0.125
$
$
$...Impose T45=T-45 for Balanced Layup
DLINK,1,10001,0.0,1.0,10003,1.00
DLINK,2,10005,0.0,1.0,10007,1.00
DLINK,3,10009,0.0,1.0,10011,1.00
DLINK,4,10013,0.0,1.0,10015,1.00
DLINK,5,10017,0.0,1.0,10019,1.00
DLINK,6,10021,0.0,1.0,10023,1.00
DLINK,7,10025,0.0,1.0,10027,1.00
DLINK,8,10029,0.0,1.0,10031,1.00
DLINK,9,10033,0.0,1.0,10035,1.00
$
DLINK,11,10101,0.0,1.0,10103,1.00
DLINK,12,10105,0.0,1.0,10107,1.00
DLINK,13,10109,0.0,1.0,10111,1.00
DLINK,14,10113,0.0,1.0,10115,1.00
DLINK,15,10117,0.0,1.0,10119,1.00

```

```

DLINK,16,10121,0.0,1.0,10123,1.00
DLINK,17,10125,0.0,1.0,10127,1.00
DLINK,18,10129,0.0,1.0,10131,1.00
DLINK,19,10133,0.0,1.0,10135,1.00
$
$...Relate the design variables to analysis model properties
$
$ Top Skin
DVPREL1,20001,PCOMP,29,T1
,10001,1.0
DVPREL1,20002,PCOMP,29,T2
,10002,1.0
DVPREL1,20003,PCOMP,29,T3
,10003,1.0
DVPREL1,20004,PCOMP,29,T4
,10004,1.0
DVPREL1,20005,PCOMP,28,T1
,10005,1.0
DVPREL1,20006,PCOMP,28,T2
,10006,1.0
DVPREL1,20007,PCOMP,28,T3
,10007,1.0
DVPREL1,20008,PCOMP,28,T4
,10008,1.0
...
$
$ Bottom Skin
DVPREL1,20101,PCOMP,36,T1
,10101,1.0
DVPREL1,20102,PCOMP,36,T2
,10102,1.0
DVPREL1,20103,PCOMP,36,T3
,10103,1.0
DVPREL1,20104,PCOMP,36,T4
,10104,1.0
...
$
$...Identify Analysis Responses
$
$ Weight Response for Objective
DRESP1,30000,W,WEIGHT
$
$ Responses for Failure Index
DRESP1,30001,FI,CFAILURE,PCOMP,,5,1,29
,28,3,32,4,31,5,30,20
,36,16,6,35,7,34,8,33
,18
DRESP1,30002,FI,CFAILURE,PCOMP,,5,2,29
,28,3,32,4,31,5,30,20
,36,16,6,35,7,34,8,33
,18
DRESP1,30003,FI,CFAILURE,PCOMP,,5,3,29
,28,3,32,4,31,5,30,20
,36,16,6,35,7,34,8,33
,18
DRESP1,30004,FI,CFAILURE,PCOMP,,5,4,29
,28,3,32,4,31,5,30,20
,36,16,6,35,7,34,8,33

```

```

,18
$
$ Responses for Percentage of Each Orientation
$ TZ0
DRESP2,30011,Frac45,1
,DESVAR,10001,10002,10003,10004
DRESP2,30012,Frac0,1
,DESVAR,10002,10001,10003,10004
DRESP2,30013,Frac90,1
,DESVAR,10004,10001,10002,10003
$ TZ1
DRESP2,30014,Frac45,1
,DESVAR,10005,10006,10007,10008
DRESP2,30015,Frac0,1
,DESVAR,10006,10005,10007,10008
DRESP2,30016,Frac90,1
,DESVAR,10008,10005,10006,10007
$ TZ2
DRESP2,30017,Frac45,1
,DESVAR,10009,10010,10011,10012
DRESP2,30018,Frac0,1
,DESVAR,10010,10009,10011,10012
DRESP2,30019,Frac90,1
,DESVAR,10012,10009,10010,10011
...
DEQATN 1 F(T1,T2,T3,T4)=T1*100./(T1+T2+T3+T4)
$
$ Response for Composite Allowable Strain
$ Top Skin under Compression Load, min principal strain selected
DRESP1,30101,COMSTRA,CSTRAIN,PCOMP,,10,1,29
,28,3,32,4,31,5,30,20
DRESP1,30102,COMSTRA,CSTRAIN,PCOMP,,10,2,29
,28,3,32,4,31,5,30,20
DRESP1,30103,COMSTRA,CSTRAIN,PCOMP,,10,3,29
,28,3,32,4,31,5,30,20
DRESP1,30104,COMSTRA,CSTRAIN,PCOMP,,10,4,29
,28,3,32,4,31,5,30,20
$ Bottom Skin under Tension Load, max principal strain selected
DRESP1,30105,COMSTRA,CSTRAIN,PCOMP,,9,1,36
,16,6,35,7,34,8,33,18
DRESP1,30106,COMSTRA,CSTRAIN,PCOMP,,9,2,36
,16,6,35,7,34,8,33,18
DRESP1,30107,COMSTRA,CSTRAIN,PCOMP,,9,3,36
,16,6,35,7,34,8,33,18
DRESP1,30108,COMSTRA,CSTRAIN,PCOMP,,9,4,36
,16,6,35,7,34,8,33,18
DEQATN 2 F(STR)=ABS(STR)*1000000.
DRESP2,30201,COMSTRA2,2
,DRESP1,30101
DRESP2,30202,COMSTRA2,2
,DRESP1,30102
DRESP2,30203,COMSTRA2,2
,DRESP1,30103
DRESP2,30204,COMSTRA2,2
,DRESP1,30104
DRESP2,30205,COMSTRA2,2
,DRESP1,30105
DRESP2,30206,COMSTRA2,2

```

```

,DRESP1,30106
DRESP2,30207,COMSTRA2,2
,DRESP1,30107
DRESP2,30208,COMSTRA2,2
,DRESP1,30108
$
$ Responses for Flutter Constraints
DRESP1,30301,FLUTTER,FLUTTER,,,,,999
,1,2,4
SET1,999,1,THRU,5
FLFACT,4,500000.
DRESP2,30302,GDAMP,3
,DRESP1,30301
DEQATN 3    F(D1)=(D1-0.03)/0.1
$
$
$...Identify the constraints
$
$ Constraints for Tsai-Wu Failure Index
DCONSTR,40001,30001,,1.0
DCONSTR,40001,30002,,1.0
DCONSTR,40001,30003,,1.0
DCONSTR,40001,30004,,1.0
$
$ Constraints for Percentage of Orientation
DCONSTR,40001,30012,10.0
DCONSTR,40001,30013,10.0
DCONSTR,40001,30015,10.0
DCONSTR,40001,30016,10.0
DCONSTR,40001,30018,10.0
DCONSTR,40001,30019,10.0
DCONSTR,40001,30021,10.0
...
$
$ Constraint for Allowable Strain
DCONSTR,40001,30201,,4000.0
DCONSTR,40001,30202,,4000.0
DCONSTR,40001,30203,,4000.0
DCONSTR,40001,30204,,4000.0
DCONSTR,40001,30205,,4000.0
DCONSTR,40001,30206,,4000.0
DCONSTR,40001,30207,,4000.0
DCONSTR,40001,30208,,4000.0
$
$...Identify Flutter Constraints
DCONSTR,40002,30302,-1.0e20,-0.3
$
$...Optional override of design optimization parameters:
PARAM,NASPRT,1
DOPTPRM,DESMAX,20,DELX,0.5,P1,1,P2,3
ENDDATA

```